2009

Structure of the Skagit Gneiss Complex in Diablo Lake area, North Cascades, WA

Niki Everette Wintzer
San Jose State University

STRUCTURE OF THE SKAGIT GNEISS COMPLEX IN DIABLO LAKE AREA, NORTH CASCADES, WA

A Thesis

Presented to

The Faculty of the Department of Geology

San José State University

In Partial Fulfillment

of the Requirements for the Degree

Master of Science

by

Niki Everette Wintzer

December 2009

STRUCTURE OF THE SKAGIT GNEISS COMPLEX IN DIABLO LAKE AREA, NORTH CASCADES, WA

by

Niki Everette Wintzer

APPROVED FOR THE DEPARTMENT OF GEOLOGY

SAN JOSE STATÉ UNIVERSITY

December 2009

Dr. Robert B. Miller	Department of Geology
Dr. Jonathan S. Miller	Department of Geology
Dr. Ellen P. Metzger	Department of Geology

ABSTRACT

STRUCTURE OF THE SKAGIT GNEISS COMPLEX IN DIABLO LAKE AREA, NORTH CASCADES, WA

by Niki Everette Wintzer

The crystalline core of the North Cascades is part of a thick (>55 km) 96-45 Ma continental magmatic arc. The highest-grade part of the arc is the Skagit Gneiss Complex, composed mostly of partially migmatitic amphibolite-facies orthogneiss, banded biotite gneiss, and paragneiss. The typically NW-striking foliation and mostly gently SE-plunging lineation formed dominantly between 69 and 51 Ma. Four-fold generations are recorded in the study area, some of which formed from 51 to 46 Ma. The prominent upright km-scale folds are similar to Eocene folds in the southern part of the Skagit Gneiss Complex and suggest at least a short interval of regional shortening during an extended period of overall transtension. Latest ductile deformation is marked by strong subhorizontal constrictional fabrics in granodiorite, which intrudes all other major units and structures at 46-45 Ma. Microstructures record relatively low-temperature (300-400º C) and medium- to high-temperature (≥450º C) ductile deformation, which are focused in different km-scale domains. Orientations, sequences, and timing of structures are similar in the northern and southern portions of the Skagit Gneiss Complex, but structures are different in orientation and apparently do not record the switch in direction of non-coaxial shear in the central portion.

ACKNOWLEDGMENTS

Worthwhile accomplishments are never the product of solitary effort but are the product of a choir of support. Foremost I acknowledge Dr. Robert B. Miller for his guidance, time, and critical thesis reviews. I sincerely thank Dr. Ellen P. Metzger and Dr. Jonathan S. Miller for serving on my thesis committee and their valuable feedback on this thesis. The National Science Foundation (EAR-0511062) and the U.S. Geological Survey EDMAP award (08HQAG0044) provided the greatly-appreciated financial support. Stereoplots were prepared with Stereonet 6.3.3 created by Richard W. Allmendinger.

My hard-working field assistants Brad Buerer, Noah McLean, Minta Schaefer, Brett Witzel, Stephen Thomas Troy, Stacia Gordon, and Mathew Wintzer deserve ample recognition for their selfless contribution of time, energy, and sweat. I am greatly indebted to Paul Bauer, my professor, mentor, and friend; without him, I would not have fallen in love with Geology. I would like to express deep gratitude to my best friend and adventure racing partner Dr. Rebecca L. Schmeisser for her encouragement, advice, enthusiasm, loyalty, and for believing in me.

I wholeheartedly dedicate my thesis to Jesus Christ, who is the author and perfecter of my faith, and to Mathew Collings Wintzer my hero, soul mate, and husband.

TABLE OF CONTENTS

LIST OF FIGURES

Figure

LIST OF TABLES

Table

LIST OF PLATES

Plate

INTRODUCTION

Geologic Setting

North-central Washington State displays the exhumed crystalline core of the North Cascades, which provides a window into the mid- and deep crust (Misch, 1966). The crystalline core is the southernmost segment of the >1500 km-long Coast Plutonic Complex, which is the largest Mesozoic Cordilleran arc (Fig. 1) (e.g., Tabor et al., 1989; Miller et al., 2009b). Dominantly tonalitic plutons, ranging from 96- to 45 Ma, intrude terranes of arc and oceanic origin (Fig. 1) (e.g., Tabor et al., 1989; Walker and Brown, 1991; Miller et al., 2009b). Plutonism in the crystalline core of the North Cascades (Cascades core) was coeval with ductile deformation and amphibolite-facies metamorphism (e.g., Misch, 1966; Tabor et al., 1989).

During the Late Cretaceous (>96- 73 Ma), the crystalline core experienced SW-NE contraction and subsequently dextral transpression during the Late Cretaceous to early Tertiary (73-57 Ma) (e.g., Misch, 1988; Miller and Bowring, 1990; McGroder, 1991; Miller et al., 2006). Mid-Cretaceous burial of the crystalline core is attributed to intra-arc shortening resulting from final eastward suturing of the Insular and Intermontane superterranes, or increased plate coupling (e.g., Brandon et al., 1988; Whitney and McGroder, 1989; Evans and Davidson, 1999), and/or to pluton-derived magma loading (Brown and Walker, 1993). The lack of granulites, depth and

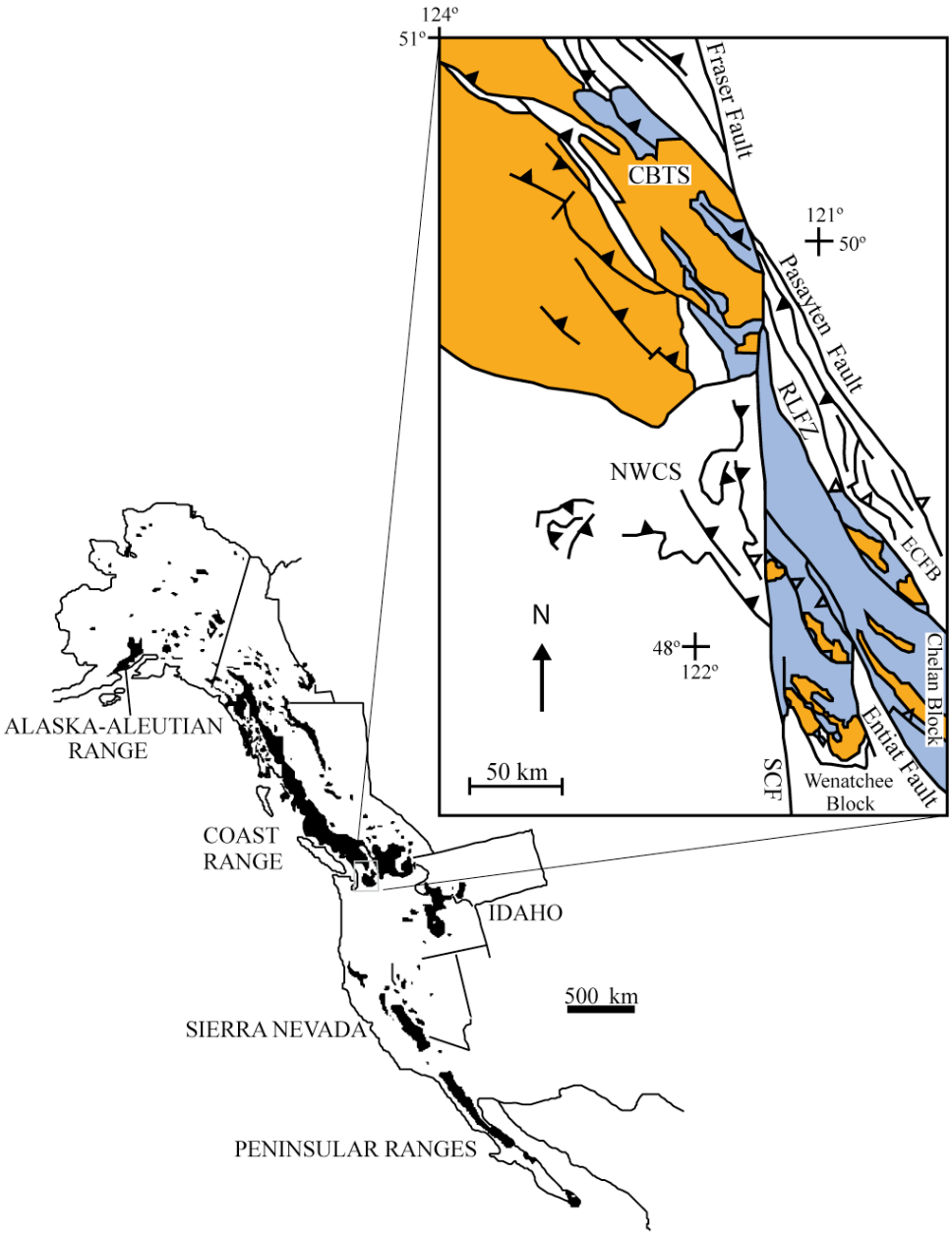

Figure 1. Map of western North American Cordillera. Arc plutons from the Mesozoic and Paleogene are emphasized. Inset map focuses on the southern Coast Ranges and North Cascades arc. Metamorphic rocks of the Cascades core are blue and Jurassic-Paleogene plutons are orange. The Coast Belt thrust system (CBTS), folds and thrusts of Eastern Cascades fold belt (ECFB), the Northwest Cascades system (NWCS), Ross Lake fault zone (RLFZ), and Cretaceous reverse faults within the Cascades core are shown. The Cascades core is offset from the main part of the Coast belt by the dextral Fraser-Straight Creek fault (SCF). Taken from Miller and Paterson (2001).

geochemistry of plutons suggest that crustal thickness was likely ≥55 km dominance of metamorphosed supracrustal rocks recording pressures of up to 12 kbar (35-40 km), (Miller and Paterson, 2001; Miller et al., 2009b).

A transtensional strain regime prevailed in the early Tertiary (<57 Ma) (Miller and Bowring, 1990; Haugerud et al., 1991; Paterson et al., 2004). The extension direction determined from ductile high-grade rocks is on average orogen-parallel (Miller et al., 2009b). The average extension direction of the shallow crust, as determined from Eocene dike swarms, is counter-clockwise (mostly 10º-30º) to the ductile stretching direction (Doran, 2009). Decoupling of deformation between the shallow and upper crust is suggested based on this disparity in extension direction (Miller et al., 2009b).

The Eocene Entiat fault divides the Cascades core into the Wenatchee block to the southwest and Chelan block to the northeast (Fig. 1) (Tabor et al., 1989; Miller et al., 2006). Magmatism is recorded from ca. 96 to 84 Ma in the Wenatchee block and ca. 91 to 45 Ma in the Chelan block. Young 50-45 Ma Ar/Ar and K-Ar hornblende and biotite dates from two domains reveal that parts of the Chelan block, including the Skagit Gneiss Complex, remained hot until the Eocene (Haugerud et al., 1991; Wernicke and Getty, 1997; Paterson et al., 2004).

The Skagit Gneiss Complex crops out as a northwest-trending belt in the northern portion of the Chelan block (Fig. 2). This antiformal complex is composed of orthogneiss, metamorphosed supracrustal rocks of oceanic and volcanic-arc origin,

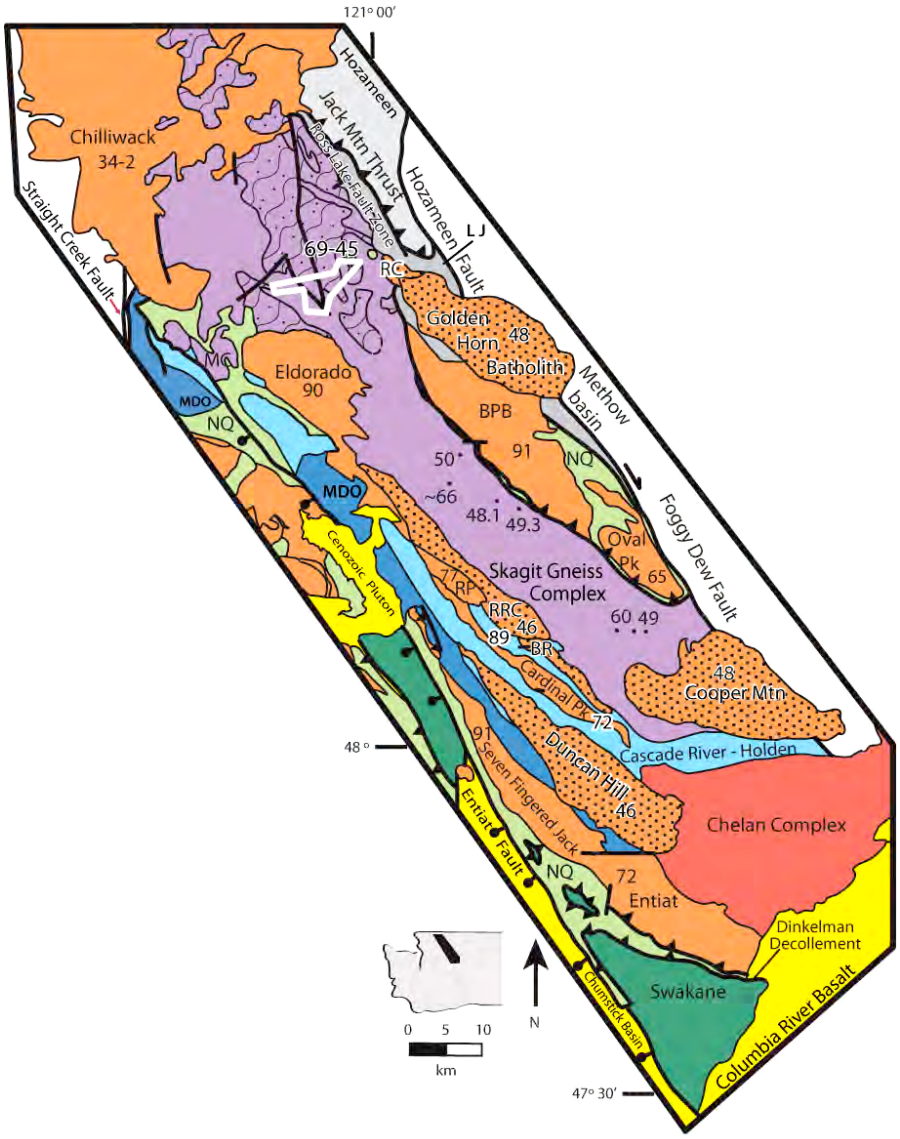

Figure 2. Simplified geologic map of the Cascades core. Terranes and plutons of the Chelan block are emphasized. Numbers are ages of plutons and inferred crystallization ages of orthogneisses in the Skagit Gneiss Complex. Combined dotted and wave pattern in Skagit Gneiss Complex represents the banded biotite gneiss component. BPB=Black Peak batholith; BR=Bearcat Ridge Orthogneiss; LJ=Little Jack phyllite and schist; MC=Marble Creek pluton; MDO=Marblemount-Dumbell Orthogneiss; NQ=Napeequa unit; RC=Ruby Creek plutonic belt; RP=Riddle Peaks gabbro; RRC=Railroad Creek pluton. Dotted pattern indicates Eocene plutons. Study area shown by white box. Crystallization ages from the Skagit Gneiss Complex are from recent U-Pb zircon dates (Shea, 2008; Michaels, 2008; N. McLean, unpub.; Gordon, 2009). Modified from Miller et al. (2009a).

trondhjemitic pegmatites, and granitic dikes; portions of the complex are migmatitic (Misch, 1966, 1968; Yardley, 1978; Babcock and Misch, 1988). Recent research revealed that the southern and central portions of the Skagit Gneiss Complex are almost entirely orthogneiss (Michels, 2008; Shea, 2008).

Zircon U-Pb analyses from leucosomes in migmatites of the Skagit Gneiss Complex at the western and eastern edges of the study area indicate at least two pulses of migmatization (69-63 Ma and 54-51 Ma), which is younger to the east (Gordon, 2009). Multiple leucosomes and mesosomes yielded monazite U-Pb dates of ca. 69 and 49-46 Ma, which implies the Skagit Gneiss Complex remained hot until the middle Eocene (Gordon, 2009). Thermobarometric data indicate that the Skagit Gneiss Complex experienced near-isothermal decompression from 8-10 kbar to 3-4 kbar at temperatures of 725-600º C in the Late Cretaceous and/or early Tertiary (Whitney, 1992a). The narrow range of pressures is consistent with the limited crustal thickness exposed in the study area (2.1 to 2.8 km), as determined from cross sections (see Plates from this study). Decompression is compatible with rapid Eocene exhumation recognized in parts of the Chelan block (Whitney, 1992a; Paterson et al., 2004; Miller et al., 2009b). The Skagit Gneiss Complex is the largest domain of hot crust exposed due to this exhumation. To the north, the Chilliwack batholith cuts the Skagit Gneiss Complex and all of its ductile structures (Misch, 1966) and is as old as 34 Ma (Tepper, 1996). Structural analysis of the Skagit Gneiss Complex is key to understanding the Cenozoic ductile deformation history of the Cascades core.

Study Area

This thesis focuses on a portion of the Skagit Gneiss Complex along Highway 20 from Ross Dam to 3 km west of Diablo Dam (Fig. 3). Excellent exposure, accessibility, and a wide range of rock types make this an ideal location to conduct a detailed study of the gneiss complex. The installation of Highway 20 created numerous road cuts that expose rock at low elevations. Surrounding topography has high to extremely high relief that only an expert mountaineer can traverse safely.

Basic geologic information was previously published about the study area (e.g., Misch, 1966, 1968; Haugerud et al., 1991), including a 1:100,000 scale geologic map (Tabor et al., 2003) and numerous detailed studies of migmatite petrogenesis (Misch, 1968; Yardley, 1978, Babcock and Misch, 1988, Whitney, 1992b, Gordon, 2009). Ample geochronological and thermobarometric data were obtained as well (Haugerud et al., 1991; Whitney, 1992a; Wernicke and Getty, 1997; Gordon, 2009), but there were only limited structural data, which are necessary for a more complete understanding of the geologic history.

This thesis involved geological mapping at a scale of 1:24,000 and 1:12,000 (Plates 1 and 2). Detailed structural data were collected at 255 stations including foliation, lineation, axial surface, and hinge line orientations where possible. Sense-of-shear from kinematic indicators was recorded and combined with the geochronological and thermobarometric data of other workers; these structural data

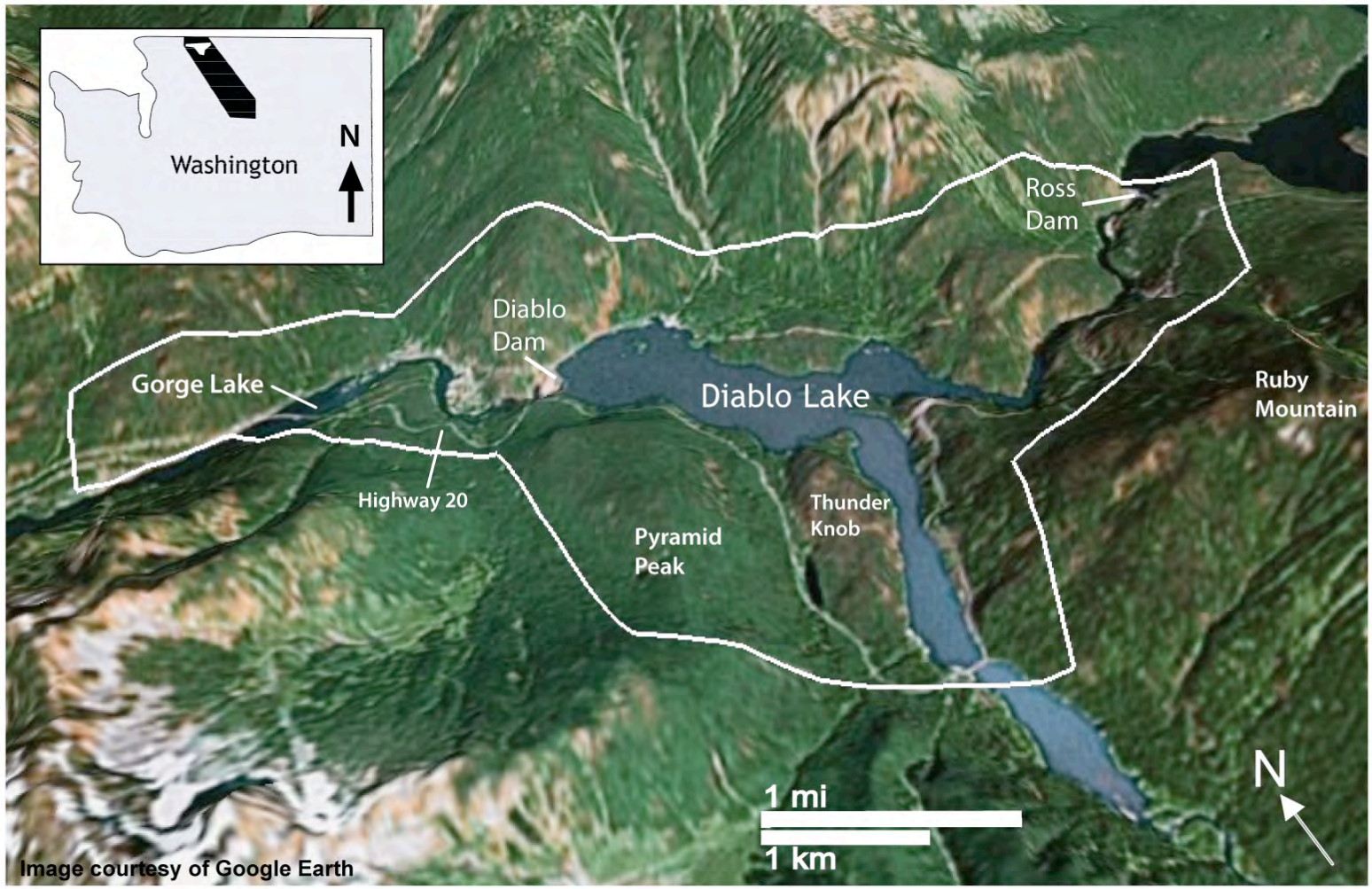

Figure 3. Outline of study area. Inset map shows the location of the study area in white and the location of Figure 2 in black. Note that the view and north arrow of the larger map is oblique.

provide insights into the deformational history and the changing strain field of the northern part of the Cascades crystalline core.

The Skagit Gneiss Complex has been termed the backbone of the North Cascades due to its overall antiformal shape (Misch, 1966; Tabor et al., 2003). The hinge zone of this regional NW-SE-trending antiform goes through the middle of the study area. Although the basic geometry of the antiform was known, little data had been collected

before this study on the smaller-wavelength folds. Thus, a major part of the research was to document the scale, geometry, and style of folds.

The crystalline core of the North Cascades was sufficiently hot to experience crustal flow (e.g., Miller et al., 2009b). Asymmetric meso- and microstructures and lineation orientations offer insights into the direction of crustal flow, and sense-of-shear was determined from kinematic indicators where possible. Approximate deformation temperatures, based on microstructures, were also determined following Passchier and Trouw (2005). Correlations between kinematic indicators, deformation temperatures, and rock age were made to evaluate the strain field in the Late Cretaceous to early Tertiary.

Migmatites in the Skagit Gneiss Complex have been studied since the 1950s and continue to be a topic of much interest (Misch, 1968; Yardley, 1978, Babcock and Misch, 1988, Whitney, 1992b, Gordon, 2009). Metamorphic differentiation and metasomatism were originally thought to be the sole cause of migmatite formation (Misch, 1966; Yardley, 1978). Geochemical, petrographic, and field evidence point to

infiltration of an aqueous fluid into the Skagit Gneiss Complex along foliation or fracture planes (Babcock and Misch, 1988). Partial in-situ anatexis was later attributed to hydrothermal fluids emanating from proximal crystallizing plutons based on CO_2-rich fluid inclusions originally sourced from water-saturated graphitic metasedimentary rocks by a chemical reaction that produces garnet+melt+CO_2-CH_4 (Whitney, 1992b). The zircon and monazite U-Pb dates (Gordon, 2009) from multiple leucosomes and mesosomes indicate two migmatization pulses (69-63 Ma and 54-51 Ma). It is thus clear that the migmatites formed over a protracted period of time and likely formed from multiple mechanisms. Building on this previous work, I semi-quantitatively estimated the distribution of migmatites at the 1:24,000 scale. The migmatite distribution map compiled for the study area was used to determine if there are correlations between age, migmatite density, and location.

ROCK UNITS

Skagit Gneiss Complex

Introduction

Metamorphosed supracrustal rocks and orthogneiss make up the Skagit Gneiss Complex, which is cut by late dacite dikes. The Diablo Lake study area is comprised of roughly 45% migmatitic orthogneiss, 35% migmatitic banded biotite gneiss, 15% Diablo Lake orthogneiss, and 5% schist, amphibolite, calc-silicate rock, and metaperidotite (Plates 1 and 2). The protolith of the banded biotite gneiss is uncertain because of its non-diagnostic mineralogy and pervasive deformation and recrystallization. Aluminosilicate minerals, such as fibrolite in the paragneiss unit, allow for protolith determination; however, they are sparse within the Skagit Gneiss Complex. The Napeequa Schist and the Cascade River Schist are considered to be the most likely protoliths of the banded biotite gneiss (Misch, 1966, 1977; Haugerud et al., 1991; Tabor et al., 2003). Amphibolite, quartzite (metachert), and siliceous schist and metaperidotite dominate the Napeequa Schist, which is considered to be Mississippian-Jurassic (Miller et al., 2009b). Biotite schist, hornblende schist, calc-silicate rock, and metaconglomerate make up the Late Triassic Cascade River Schist (e.g., Tabor et al., 1989, Miller et al., 2009b).

The metamorphosed supracrustal rocks and banded gneiss of uncertain protolith host the orthogneiss bodies that are 3 km^2 in map view. The latest orthogneiss (46-45 Ma Diablo Lake orthogneiss) crops out in larger bodies (1.5 km^2) and thick to thin sheets (5-15 m across). Older and late orthogneiss records distinctly different types of strain. Many of these bodies are shown on a geologic map of the Mount Baker quadrangle at the 1:100,000 scale (Tabor et al., 2003). Additional units were recognized in the study area and a much more detailed map was produced. All units were examined for kinematic indicators (Figs. 4 and 5). These asymmetric structures include the following: rotated plagioclase porphyroclasts and garnet porphyroblasts with mica tails, biotite "fish," oblique quartz foliation, and deflected leucosomes. Microstructures provide information about temperatures during ductile deformation (Fig. 6). Quartz grain boundary bulging and quartz ribbons with limited subgrains and recrystallization, plagioclase microfractures and deformation twins, and undulatory extinction in biotite and/or plagioclase imply a deformation temperature range of 300 to 400ºC (Passchier and Trouw, 2005). Core-and-mantle microstructures in plagioclase as well as elongated quartz subgrains and grains bounded by 120º angle faces are compatible with deformation at ≥450º C (Passchier and Trouw, 2005). Recrystallized hornblende and cummingtonite also indicate deformation at ≥500º C (Passchier and Trouw, 2005). The 40 thin sections examined in this study were analyzed for microstructures that indicate deformation temperature.

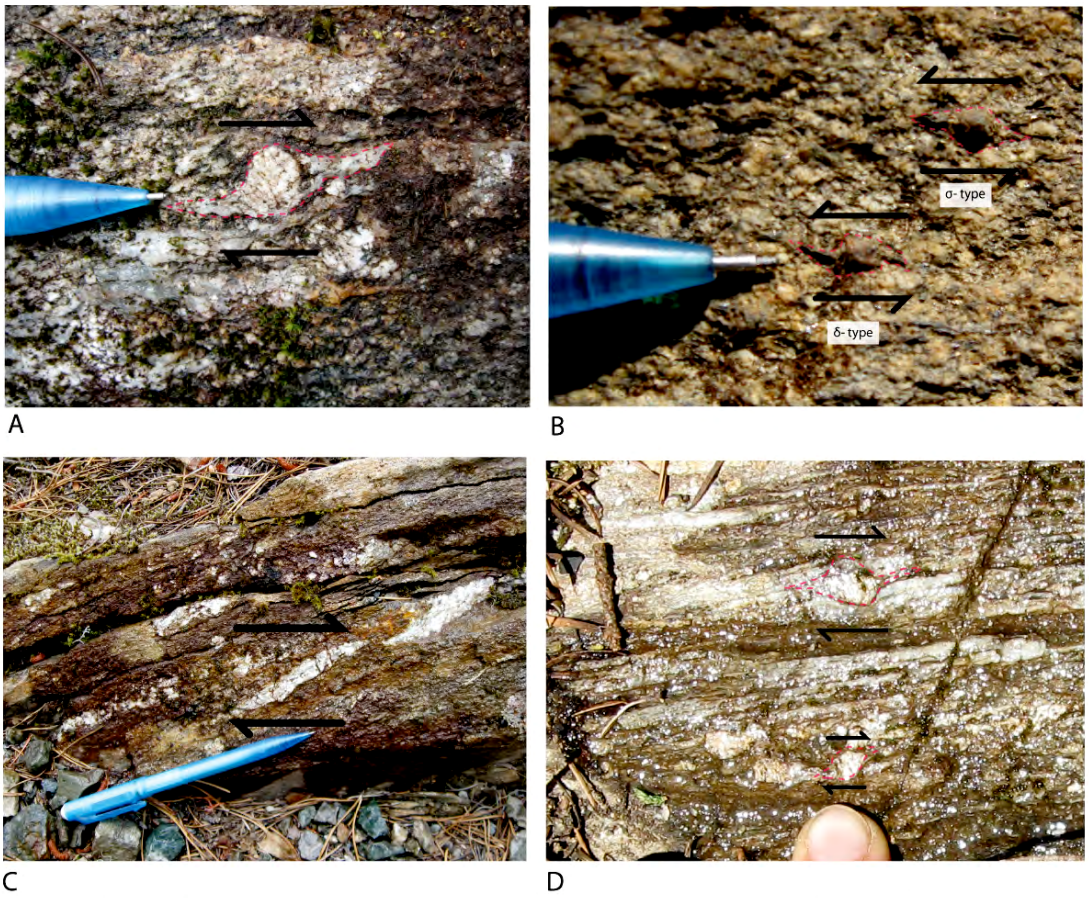

Figure 4. Field photographs of mesoscale kinematic indicators. Rock type for all photographs is banded biotite gneiss. (A) Rotated plagioclase porphyroclast; (B) sigma (σ) and delta (δ) type garnet porphyroblasts; (C) leucosome deflected by two shear zones; and (D) sigma (lower) and delta (upper) type plagioclase porphyroclasts.

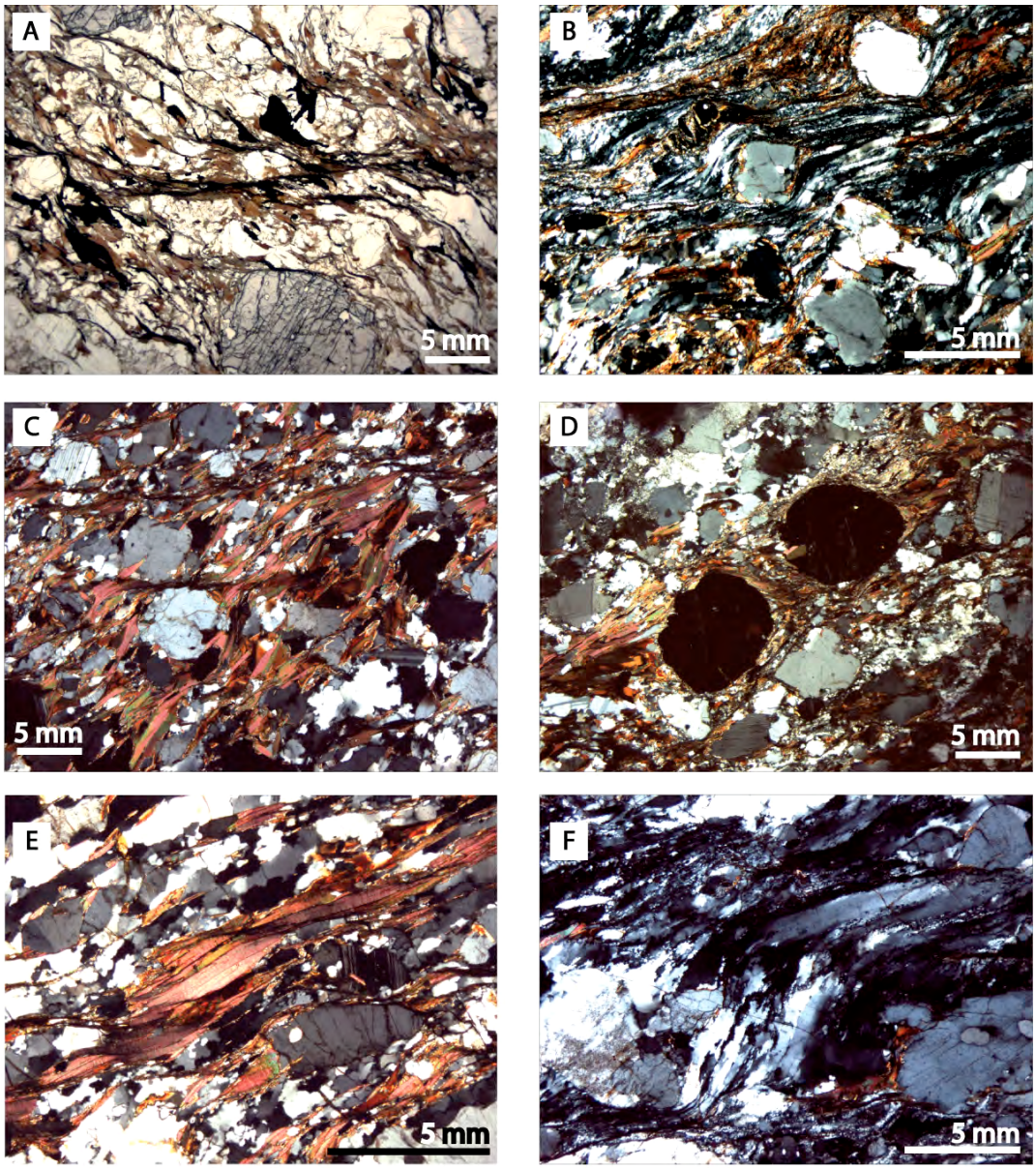

Figure 5. Photomicrographs of microstructures that give sense-of-shear. A is top-to-the-left and under plane polarized light; B through F are top-to-the-right and under cross polarized light. Banded biotite gneiss and paragneiss contain the following: (A) S-C fabric (plane polar); (B) asymmetric plagioclase porphyroclast with tails of biotite and quartz; (C) asymmetric plagioclase porphyroclasts, S-C surfaces, and biotite" fish"; (D) garnet porphyroblasts with asymmetric biotite tails; (E) biotite "fish"; and (F) oblique quartz in ribbons.

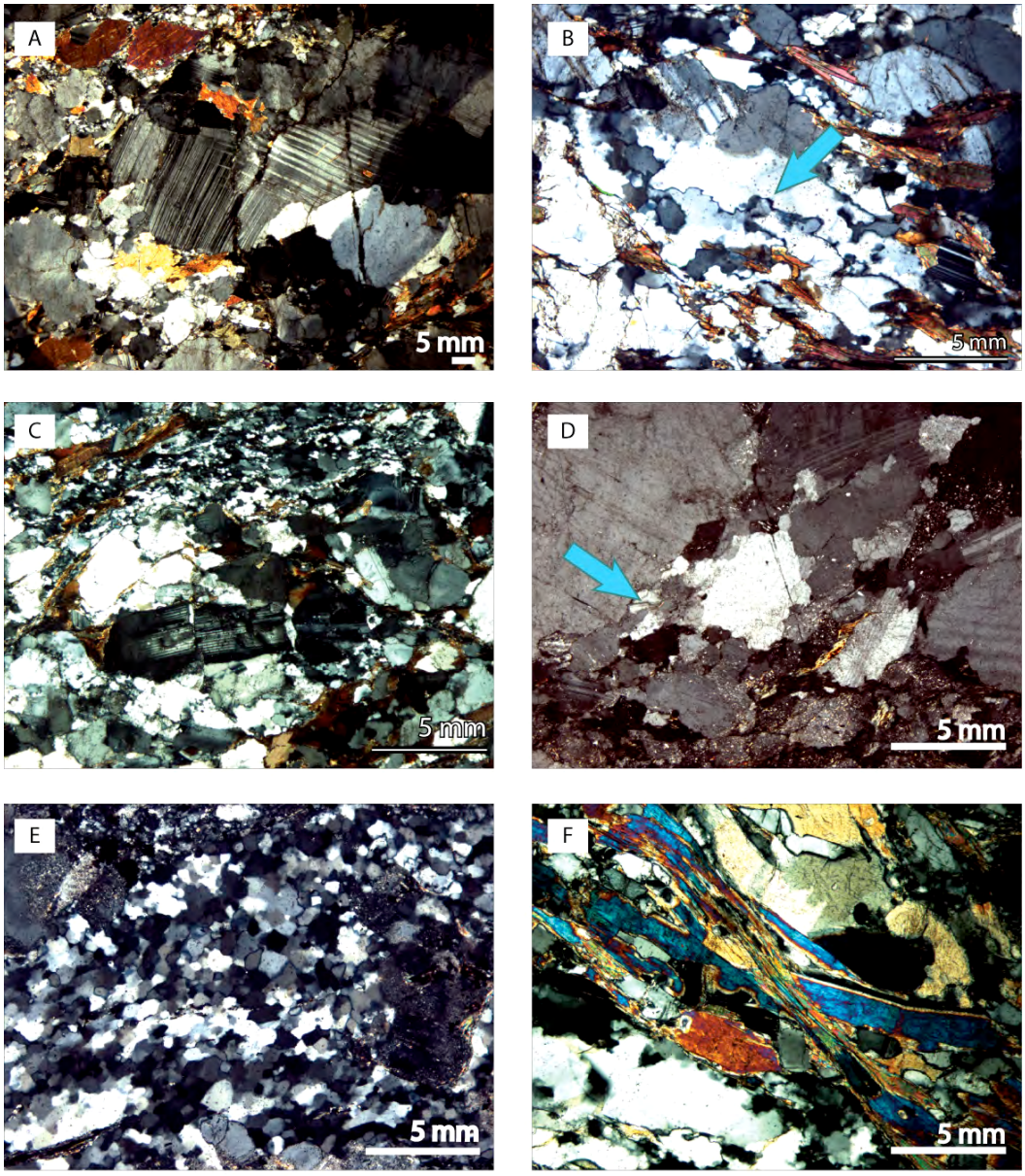

Figure 6. Microstructures that give deformation temperature. A through C are lower-temperature microstructures (300-400°C); D through F are higher-temperature microstructures (≥450°C). (A) Slightly bent plagioclase grain with deformation twins; (B) quartz subgrains and bulging between grains (arrow points to a bulge); (C) microfractures in plagioclase; (D) plagioclase core and mantle structure (arrow point to recrystallized mantle); (E) 120° angle grain boundary junctions between recrystallized quartz grains; and (F) cummingtonite recrystallized in C-surface.

Orthogneiss

Orthogneiss within the study area was previously categorized as quartz diorite orthogneiss, mafic orthogneiss, or coarse-grained banded gneiss and described as porphyritic and/or trondhjemitic (Misch, 1966; Tabor et al., 2003). Most orthogneiss in the study area is tonalitic; however, the Diablo Lake orthogneiss is mostly granodioritic. The tonalitic orthogneiss bodies are variably migmatized. Percent leucosome of the outcrop ranges from 0% to 50%; leucosomes are concordant and discordant to foliation at the millimeter to meter scale. The orthogneiss is divided into four main units based on locality and modal mineralogy; they are named hornblende tonalite gneiss, hornblende ± garnet gneiss, hornblende-cummingtonite-garnet gneiss, and Diablo Lake orthogneiss.

Hornblende Tonalite Gneiss. Located northeast of Diablo Lake (Plates 1 and 3), this ≥ 4.5 km^2 orthogneiss body contains hornblende and lacks cummingtonite and garnet found in other orthogneiss bodies within the study area. The primary modal mineral assemblage consists of plagioclase-quartz-hornblende-biotite (42%, 32%, 16%, and 10%, respectively); accessory amounts of zircon, oxides (magnetite and/or ilmenite), and secondary epidote, chlorite, and sericite are present. Grain size is fine to medium.

Foliation and lineation are defined by biotite, quartz, and hornblende. This orthogneiss shows equally intense foliation and lineation; however, the overall intensity of foliation and lineation varies from outcrop to outcrop. Orthogneiss and host rock foliation and lineation are concordant. Contacts of the orthogneiss with the

host rock are marked by 1 to 3 m-wide zones of alternating sheets of orthogneiss and banded biotite gneiss.

Plagioclase has deformation twins, undulatory extinction, and microfractures, and ranges from 0.5 to 3 mm in average length. Quartz displays subgrains and ribbons. As indicated by the microstructures such as quartz grain boundary bulging and lack of plagioclase recrystallization, deformation occurred at temperatures of 300-400º C (Passchier and Trouw, 2005). Other microstructures, including S-C surfaces and biotite "fish," reveal sense-of-shear in this unit.

Hornblende ± Garnet Gneiss. Located around Pyramid Peak, southwest of Diablo Lake (Plates 1 and 3), this unit has a homogenous texture. Foliation and lineation are of equal intensity and fabric intensity is similar amongst different outcrops. Contacts with the host banded biotite gneiss are sharp with a narrow, 1 m-wide zone of alternating banded biotite and orthogneiss. The younger Diablo Lake orthogneiss sharply cuts through the central portion of the hornblende ± garnet orthogneiss.

The primary mineral assemblage is plagioclase-quartz-hornblende-biotite ± garnet (50%, 40%, 6%, 2%, and 2%, respectively) with accessory zircon, and oxides (magnetite and/or ilmenite), and secondary chlorite and sericite. Grains are medium to coarse, and foliation and lineation are defined by quartz, biotite, and hornblende. Plagioclase grains have deformation twins, undulatory extinction, and core-and-mantle microstructures, and range in average length from 0.5 to 3 mm. This well-developed core-and-mantle structure and polygonal mosaic of quartz imply deformation

temperature is ≥450º C (Passchier and Trouw, 2005). Oblique quartz foliation and biotite-defined shear bands offer kinematic direction. In one locality, three 0.5 m pockets of orthogneiss are suspended within a 3 m wide leucosome layer.

Hornblende-Cummingtonite-Garnet Gneiss. This ≥6 km^2 orthogneiss body is exposed in the eastern and southeastern portions of the study area (Plates 1 and 3, and Fig. 3). Foliation and lineation are defined by quartz, biotite, and cummingtonite; fabric intensity varies from weak to moderate at different outcrops. Grains are fine to coarse, and distribution of the various-sized grains is uneven. There is considerable textural variation within this unit. Contacts are sharp with the surrounding banded biotite gneiss and "metagraywacke." A few related meter-scale orthogneiss sheets lay within the "metagraywacke" west of the main orthogneiss mass along Highway 20. Misch (1977) interpreted these sheets as tectonic slices cut from the larger mass and incorporated into the host rock; the slices were later recrystallized. Alternatively, they may be intrusive sheets, which because of their competence, localized higher strain in the adjacent well-layered gneisses (R.B. Miller, written communication).

The primary mineral assemblage is plagioclase-quartz-biotite-cummingtonite-hornblende ± garnet (45%, 35%, 10%, 4%, 4%, and 2%, respectively); the accessory minerals are zircon, clinopyroxene, allanite, sphene, and oxides (magnetite and ilmenite). The secondary minerals epidote, chlorite, and prehnite indicate retrograde greenschist to prehnite-pumpellyite facies conditions. Mineral modes from my thin sections indicate the orthogneiss is tonalitic; previous workers have reported that some of the orthogneiss is dioritic (Misch, 1968; Tabor et al., 2003).

A number of garnets have sieve texture, which may represent rapid growth (Whitney, 1992a). Plagioclase-dominated coronas around a few garnets may indicate rapid decompression (e.g., Whitney, 1992a; Stowell and Stein, 2005). Foliation wraps around garnets indicating pre- or syn-tectonic growth. Plagioclase has deformation twins, undulatory extinction, bent grains (through angles of 25º), and core-and-mantle structure, and ranges in average length from 0.23 to 7 mm. The grains are also highly sericitized. Quartz subgrains bounded by 120º angle faces and highly elongate quartz ribbons are common. Biotite and cummingtonite define S-C surfaces and "fish," which provide sense-of-shear. The recrystallized cummingtonite in the C-surfaces indicates deformation at ≥500º C or higher (Passchier and Trouw, 2005).

U-Pb dating of zircon yielded a date of 67 Ma for this unit, which was interpreted as the age of igneous crystallization (Mattinson, 1972). Subsequent U-Pb zircon analysis was performed by Hoppe (1984), and in conjunction with Sm-Nd data, yielded an inferred igneous crystallization age of 69 Ma. Ar/Ar hornblende and biotite cooling dates of 47 Ma and 45 Ma indicate rapid cooling and presumably exhumation of this orthogneiss (Wernicke and Getty, 1997).

Banded Biotite Gneiss

The banded biotite gneiss was described as plagioclase porphyroblastic gneiss and lit-par-lit gneiss by Misch (1966, 1968, 1977). The Napeequa Schist and/or the Cascade River Schist (Fig. 2) are considered potential protoliths for the banded biotite

gneiss as described earlier (Misch, 1966, 1977; Haugerud et al., 1991; Tabor et al., 2003). Foliation and lineation are defined by quartz and mica, and their intensities are roughly equal. One locality north of Diablo Dam displays pervasive rodding where lineation is significantly stronger than foliation. Grains are fine to coarse. Banding of relatively mafic and felsic layers on the millimeter to tens-of-centimeters scale is diagnostic of this unit, which may be due to minimal segregation during metamorphism and deformation. Plagioclase porphyroclasts, some of which are asymmetric, are visible at the mesoscale. Leucosomes are concordant and discordant at millimeter to meter scale. Percent leucosome of individual outcrops typically ranges from 5 to 50%.

Plagioclase-quartz-biotite-garnet ± cummingtonite is the modal mineral assemblage with accessory muscovite, apatite, zircon, oxides (magnetite and/or ilmenite), and sparse secondary sericite. Average length of plagioclase grains ranges from 0.5 to 5 mm. Garnet porphyroblasts range from 1- 6 mm in diameter. Sieve texture is present in garnets. Highly elongate quartz ribbons (aspect ratio of 7:1) imply deformation under high strain rates and/or a low temperature (Passchier and Trouw, 2005). Deformation twins, subtle undulatory extinction, and cracked grains of plagioclase, and lack of recrystallization suggest that the deformation temperature for at least much of this unit is 300-400º C. Oblique quartz foliation, mica "fish," and plagioclase porphyroclasts with asymmetric biotite tails all indicate sense-of-shear.

Paragneiss

Metapelite. These rocks form bodies that are roughly 25 to 200 m across, which subtly transition into the surrounding banded biotite gneiss. Ample garnet porphyroblasts and plagioclase porphyroclasts are visible in fresh surfaces and in discrete millimeter-scale felsic and mafic layers. Leucosomes occur concordant and discordant to layering and foliation, and are commonly folded. Grain size is fine to medium. Quartz and mica define foliation and lineation.

The dominant mineral assemblage is plagioclase-quartz-biotite-muscovite ± garnet ± fibrolite ± rutile ± magnetite ± ilmenite. Aluminosilicate minerals are diagnostic of this rock unit and have only been recognized in thin section (Fig. 7) (Whitney, 1992a). Sillimanite (fibrolite) is present in the western, central, and eastern portions of the study area. Metapelite occurs as m-scale pockets in banded biotite gneiss. The central and eastern localities, which were discovered during this study, contain only fibrolite and lack garnet, thus precluding thermobarometry. Sillimanite-bearing paragneiss in two other localities west of Diablo Dam contains garnet and yields temperatures of 650-725º C and pressures of 8-10 kbar (Whitney, 1992a).

Sericite is pervasive in plagioclase grains, and chlorite replaces biotite in C-surfaces in the fibrolite-bearing samples. The average length of plagioclase grains ranges from 2 to 5 mm. Foliation wraps around the garnets indicating that the garnets are pre- or syn-tectonic. Asymmetric porphyroblasts are apparent at the mesoscale.

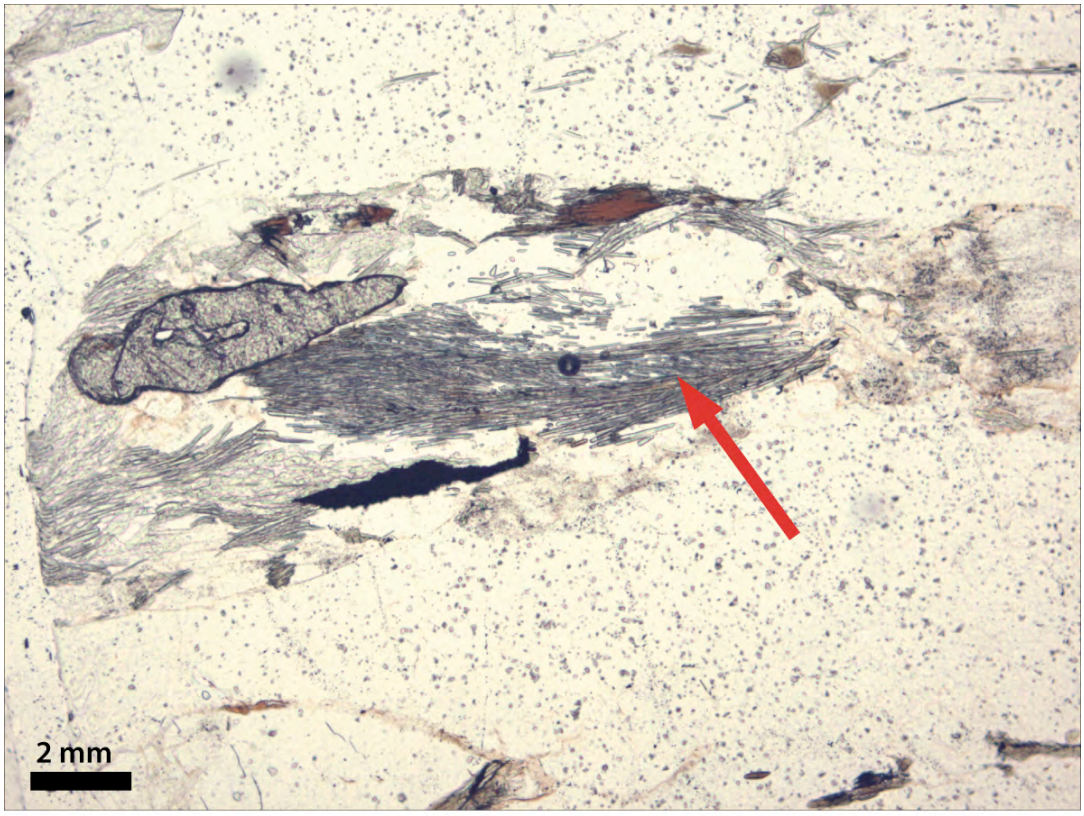

Figure 7. Fibrolite (fibrous sillimanite) under plane polarized light. Epidote is the high-relief mineral to the upper left of the sillimanite.

At the microscale, numerous mica grains are deformed into "fish." Poikiloblastic plagioclase grains with deformation twins have asymmetric tails. Elongate quartz grains are oriented obliquely to foliation. These microstructures offer sense-of-shear. Latest ductile deformation temperature was probably 300-400º C, as quartz recrystallized, but plagioclase did not. Zircon grains from the paragneiss leucosomes in the western locality were dated at 69 to 63 and are interpreted to represent one of two migmatite pulses recorded in the study area (Gordon, 2009). Monazite U-Pb dates from the metapelite are interpreted to record prograde metamorphism at around 69 Ma to 49-46 Ma (Gordon, 2009).

"Metagraywacke" Gneiss. Both localities of "metagraywacke" are in the eastern portion of the study area and are in sharp contact with hornblende-cummingtonite-garnet gneiss (Plate 1). The thickness of this unit varies from 0.5 to 1.5 km. There are sharply bounded felsic and mafic layers. Felsic layers are on the millimeter to centimeter scale and display numerous plagioclase porphyroclasts. Grain size is fine to medium and the rocks are equigranular. Plagioclase-quartz-biotite-cummingtonite-hornblende-garnet- zircon ± staurolite ± magnetite ± ilmenite ± epidote is the mineral assemblage for this unit. Plagioclase is recrystallized to a mosaic of grains ranging from 0.5 to 3 mm in length, and deformation temperature thus reached ≥450º C (Passchier and Trouw, 2005).

The term "metagraywacke" was first used by Misch (1968) and continued by Whitney (1992a) and is based on the high Mg content implied by cummingtonite. Also, mineral modes are consistent with known immature volcanic-derived sediments.

Thus, it is considered reasonable to refer to this unit as a "metagraywacke" according to Whitney (1992a), but the bulk mineral mode is also compatible with a dacitic protolith.

Biotite-Cummingtonite Schist. This unit occurs at only one locality within the study area, and the contact is sharp with the surrounding hornblende-cummingtonite-garnet gneiss. The outcrop, which is 10 m across, is highly weathered and eroded. Lighter and darker layers consisting of different amounts of plagioclase, quartz, and biotite, with and without cummingtonite, alternate on the centimeter scale. The high biotite content and strong foliation and lineation distinguish this unit. The high percentage of biotite also implies that the protolith was sedimentary.

Foliation and lineation are roughly equal in intensity and are defined by quartz, biotite, and cummingtonite. Accessory muscovite and oxides and secondary sericite are present. Deformation twins and undulatory extinction are typical of the plagioclase, and quartz grains are highly elongate with visible subgrains. These features suggest that late ductile deformation occurred at temperatures of 300-400º C. Sense-of-shear indicators include mica "fish" and plagioclase porphyroclasts with asymmetric biotite tails.

Calc-silicate Rock and Marble

Outcrops of calc-silicate rock occur northeast of Ross Dam and east-southeast of Diablo Dam along Highway 20 (Plates 1 and 2) (Misch, 1977; Tabor et al., 2003), and are roughly 50 m and 7 m across, respectively. Grain size is fine to very fine; a

sugary texture is present in a few places. The Highway 20 body was interpreted by Misch (1977) as a mobilized dike that was emplaced into wall rock; he inferred that this body is a recrystallized mylonite that contains cataclastic fragments of gneiss. Minor diopside and grossularite occur as suspended grains within the calc-silicate, and immature limestone is likely the protolith (Misch, 1968). Both outcrops represent rare metamorphosed calcareous sedimentary rocks in the Skagit Gneiss Complex.

Amphibolite

Amphibolite crops out north of Gorge Lake in the western portion of the study area and probably extends across the lake in areas that are unmapped. This unit was previously mapped and extends along strike at least 33.2 km northwest of the study area (Tabor et al., 2003). Two additional localities were mapped as part of this project (Plates 1 and 2), which are tabular bodies with NW-striking foliation concordant to the previously mapped body. Protoliths of the amphibolites are both meta-sedimentary and meta-igneous, the former of which is indicated by a relative abundance of biotite and schistose texture according to Misch (1968). A meta-igneous protolith is indicated by relict zoning in the hornblende (Misch, 1968).

A typical mineral assemblage includes plagioclase-amphibole-biotite-quartz ± garnet ± cummingtonite ± hornblende ± diopside (Misch, 1968). Painstaking care was taken by Misch (1968) to document the zoning of the plagioclase and modal mineral variation of the amphibolites, along with all Skagit Gneiss Complex units, to gain

insight into the metamorphic history. Grain size ranges from medium to coarse. Foliation and lineation are defined by hornblende and cummingtonite. Leucosomes cut the amphibolite and each other and range from 1 to 7 cm in thickness.

Migmatite

Medium-grained to pegmatitic leucosomes, dominantly trondhjemitic, form bodies that are both concordant and discordant to the main foliation in the mesosome and are more resistant to weathering than other compositional layers. Many of the leucosomes are only weakly foliated. A few localities contain mylonitic leucosomes. Thickness of the leucosomes typically ranges from 1 cm to 1.5 m. Leucosomes are present in all units of the Skagit Gneiss Complex except for the calc-silicate rock and the Diablo Lake orthogneiss. The leucosome morphology varies significantly and includes stromatic, ptygmatic, boudinaged, and pegmatitic types (see Misch [1968] for detailed descriptions). Boudins in leucosomes range in width from 0.5 cm to 1 m. Saddle reefs occur at 7 localities within banded biotite gneiss and range from 0.5 to 3 m in width.

Plagioclase-quartz-biotite ± garnet is the modal mineral assemblage. Garnet porphyroblasts range in diameter from 1 to 3 mm; they were found at only 7 localities. These garnets are inclusion-free and interpreted to be peritectic as they likely formed during a partial melting reaction (Whitney, 1992b). Core-and-mantle structure of plagioclase indicates recrystallization and a deformation temperature of ≥450º C.

The 68 Ma hornblende-cummingtonite-garnet orthogneiss contains mostly folded leucosomes, but there are a few locations of weakly foliated and non-folded leucosomes in the most northwestern-most portion of this unit along Highway 20 (Plate 1). The host orthogneiss may have shielded the leucosomes from folding. At each possible station, leucosome concentration was recorded. Leucosomes account for 5 to 45% of the outcrop volume. These values were compiled on a map (Fig. 8) that reveals domains of higher, moderate, and lower leucosome concentration (>20%, 20-5%, and <5%). There is no obvious correlation between percent leucosome and rock type. This observation suggests that all major units were equally susceptible to migmatization, which is not compatible with the range of modal minerals in the different units, or that some of the leucosomes were injected from a significant depth to the presently exposed crustal level.

Diablo Lake Orthogneiss

Although briefly mentioned, these rocks were not previously mapped as a separate unit, and were referred to informally as late-lineated granite (e.g., Haugerud, 1991) or lumped with regional orthogneiss units (Misch, 1968, 1977). Whole-rock Rb-Sr analysis of this unit yielded a 45 ± 3 Ma date from a sample locality southeast of Diablo Dam (Babcock et al., 1985), and a recent U-Pb zircon analysis yielded a 46 Ma date for a sample taken <5 km to the north (Gordon, 2009). I use the name Diablo Lake orthogneiss due to the proximity of many of these rocks to Diablo

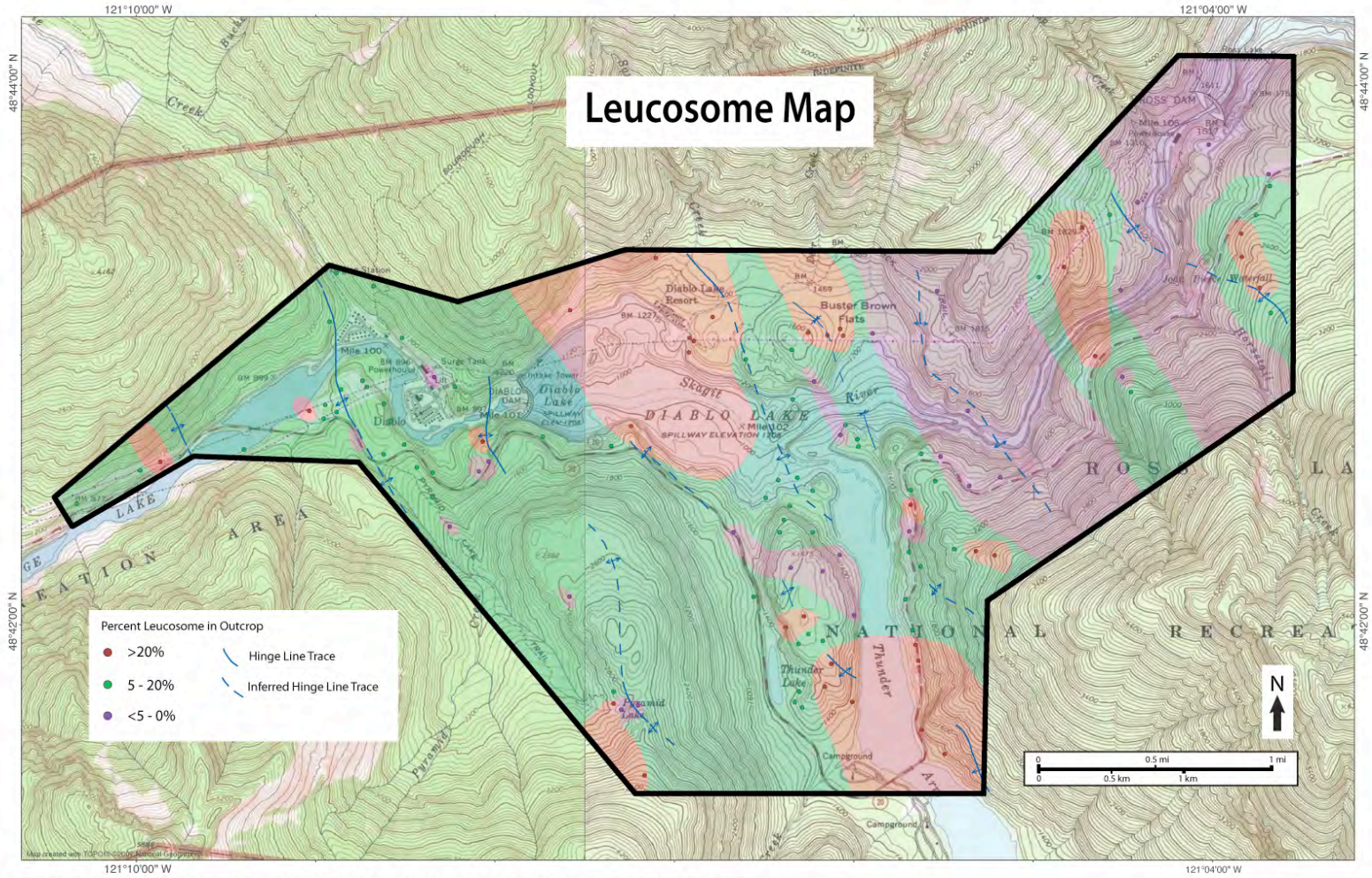

Figure 8. Leucsomes in migmatites mapped according to concentration.

Lake. This study revealed the Diablo Lake orthogneiss to be more voluminous than previously documented. The orthogneiss crops out as a 1 km^2 body in the center of the study area, as dikes in western and eastern portions, and as irregularly-shaped masses in a few places 1 throughout the study area. Dikes of this unit range in thickness from 0.5 to 18 m (Plates 1 and 2).

The Diablo Lake orthogneiss forms prominent outcrops. Grains are medium to coarse, mineral lineation is prominent, and foliation is significantly weaker than lineation or absent. The Diablo Lake orthogneiss has elongate quartz grains (7:1 on average) indicating solid-state deformation. Lineation (and foliation) is defined by quartz, biotite, and plagioclase.

Most of the orthogneiss is granodiorite; the mineral assemblage includes plagioclase-quartz-biotite-orthoclase ± hornblende. Misch (1968) also reported accessory amounts of muscovite, sphene, allanite, and oxides (magnetite and/or ilmenite). Secondary sericite and chlorite are present in moderate amounts. Average length of plagioclase grains range from 0.5 to 8 mm. Potassium feldspars commonly show relict zoning (Misch, 1977), and myrmekitic texture is present but sparse. Orthoclase grains are perthitic and fractures are common. Plagioclase shows relict compositional zoning, deformation twins, and undulatory extinction. Biotite displays undulatory extinction. The lack of feldspar recrystallization indicates deformation temperature at 300-400º C.

Felsic Dikes

These dikes occur in a main western cluster and one eastern location and cut orthogneiss and biotite gneiss. Dike widths are 20 to 100 cm. Outcrops of this unit are prominent and resistant to weathering as compared to its host gneiss. Grains are fine to coarse. The felsic dikes, which are mostly granodioritic, cut the Diablo Lake orthogneiss. Foliation and lineation of roughly equal intensity are defined by quartz and mica; however, overall deformation intensity is significantly weaker than the Diablo Lake orthogneiss. These dikes are thus given an igneous rather than a metamorphic name and are not grouped within the Skagit Gneiss Complex.

The mineral assemblage is plagioclase-quartz-potassium-feldspar ± biotite ± muscovite ± magnetite ± ilmenite. Potassium feldspar occurs as microcline and orthoclase. Plagioclase is pervasively sericitized and displays relict zoning, undulatory extinction, and cracks. Oblique quartz foliation is defined by extremely fine (0.5 mm in length) grains with aspect ratios ranging from 3:1 to 5:1. Rotated plagioclase porphyroclasts with micaceous tails and quartz-defined shear bands offer kinematic direction. Based on microstructures, deformation temperature was 300-400º C. The very low color index distinguishes these felsic dikes from the Diablo Lake orthogneiss.

Dacite Dikes

In the center of the study area, dacite dikes intrude banded biotite gneiss and probably the Diablo Lake orthogneiss (Plate 1). These dikes form prominent outcrops. Fresh rock faces reveal an aphanitic matrix with phenocrysts of feldspar and amphiboles. Phenocrysts are medium grained and subhedral to euhedral. There is no deformational fabric in this rock, which along with the intrusive relations suggests that this unit is the youngest in the study area (<46 Ma). Plagioclase-quartz-hornblende-cummingtonite and accessory oxides define the mineral assemblage. Secondary sericite and chlorite are sparse. Plagioclase is zoned. Cummingtonite has characteristic polysynthetic twinning, and some grains have thin hornblende rims. The fine-grained matrix minerals are indiscernible, except for a few amphibole grains. The coeval occurrence of cummingtonite and hornblende, which is based on optical identification in this study, is very rare and suggests the magma had a relatively low-temperature and high partial-water pressure (Geschwind and Rutherford, 1992).

STRUCTURAL ANALYSIS

Introduction

Significant insight into the deformational history of the mid- to deep crust can be gained from structural analysis of deeply exhumed crystalline rocks. In this study, foliation, lineation, fold measurements, and evaluation of kinematic indicators combined with cross-cutting relationships and absolute dating are effective tools to unravel the local and regional deformational history. The structural data collected provide information about the strain regime at the time of deformation. Additionally, cross-cutting relationships combined with geochronological data elucidate deformational "episodes." In an effort to better understand the deformation history of the Skagit Gneiss Complex, foliation, lineation, axial plane, and hinge line orientations were measured and analyzed.

Brittle structures are common in the map area, but were not analyzed as part of this study. The most prominent brittle structure is the steeply dipping Thunder Lake fault, which trends roughly N-S through the central portion of the study area (Plates 1 and 2) (e.g., Tabor et al., 2003), and has uncertain displacement. Numerous outcrop-scale faults reveal a complex pattern (Clay and Miller, 2008).

Foliation

The dominant foliation strikes NW and dips mostly moderately to steeply in the Skagit Gneiss Complex. Mean average strike is 346º and dips for two maxima, on a lower hemispheric equal area stereonet plot of poles to all foliations (n=223), are 43º NE and 35º SW (Fig. 9). There are more NE than SW dipping foliation measurements. The poles to foliation form a moderately well-defined girdle that is interpreted to represent the regional antiform (Fig. 9). The pole to the girdle is 19º to 150º. The scatter of some data points away from the girdle indicates that the regional fold is not cylindrical.

The foliation map pattern (Plate 1) reveals nine, km-scale folds; most hinge lines plunge shallowly to the SE and a few plunge shallowly to the NW. Most of these folds are upright. Curvature of the hinge lines in map view indicates that these folds are non-cylindrical. The km-scale folds have a similar trend to the regional antiform that characterizes the overall structure of the Skagit Gneiss Complex and are likely parasitic to this regional structure.

Foliation and lineation are defined by quartz, biotite, and amphiboles in outcrop and thin section. Fabric intensity is strong and consistent throughout the banded biotite gneiss and metapelites with a few areas of higher strain. Orthogneisses show the weakest foliation of the gneiss units. In the orthogneisses, strain is partitioned, as some outcrops show significantly stronger foliation and lineation than

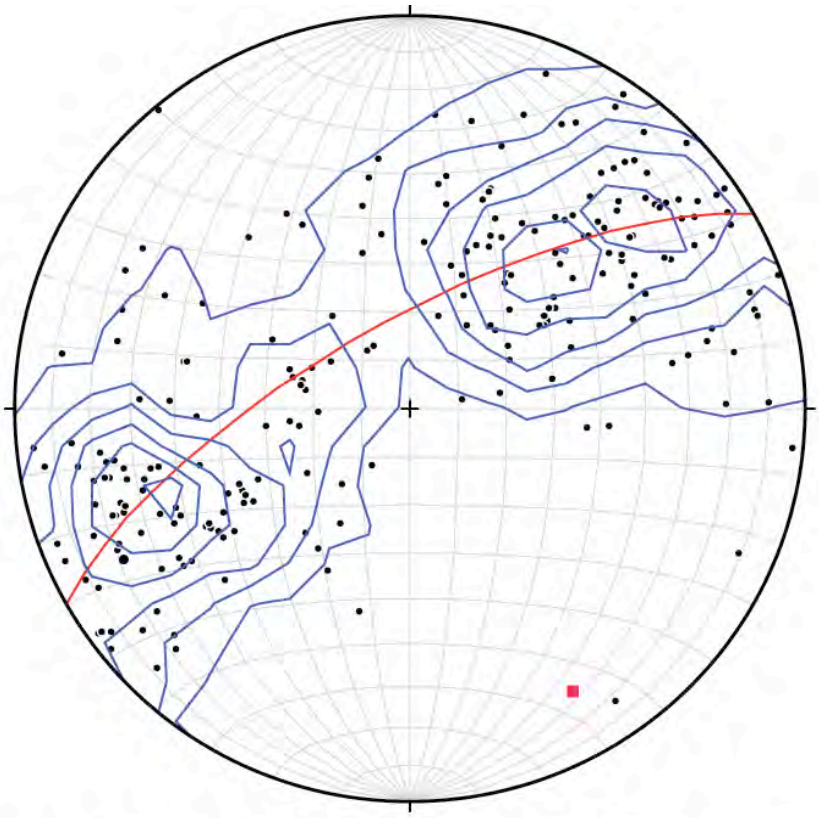

Figure 9. Stereonet plot of poles to foliation measurements (n=223). The pole to the girdle (red square) defined by foliations is 19° to 150º. Contour interval is 2.0 σ following the method of Kamb (1959), which is used in all subsequent plots with contours.

others. Some of the strongest orthogneiss fabric is the mineral lineation in the 46-45 Ma Diablo Lake orthogneiss.

Lineation

Mineral lineations, which are defined by amphiboles, biotite, and quartz grains and aggregates of these minerals, plunge shallowly to moderately and mostly trend SE or NW in the Skagit Gneiss Complex. A lower hemispheric stereonet plot of lineation measurements (n=236) indicates a well-defined maxima of 14º to 145º (Fig. 10). The relatively few NW-plunging lineations occur mainly in a domain in the northern section of the study area. A subtle culmination is thus suggested by the pattern of lineation plunges. The lineations dominantly trend parallel to subparallel to the foliation strike and are roughly the same direction throughout all units regardless of the age of the rock. The relative degree of intensity between foliation and lineation varies amongst units. In the Diablo Lake orthogneiss, lineation is much stronger than foliation, which makes foliation difficult to measure in most places. In contrast, banded biotite gneiss, paragneiss, amphibolite, felsic dikes, and all orthogneisses display roughly equal intensity of foliation and lineation. Leucosomes in migmatites have variable foliation intensity and are generally less well lineated. Along Highway 20, the sparse calc-silicate rock and marble show little to no foliation or lineation;

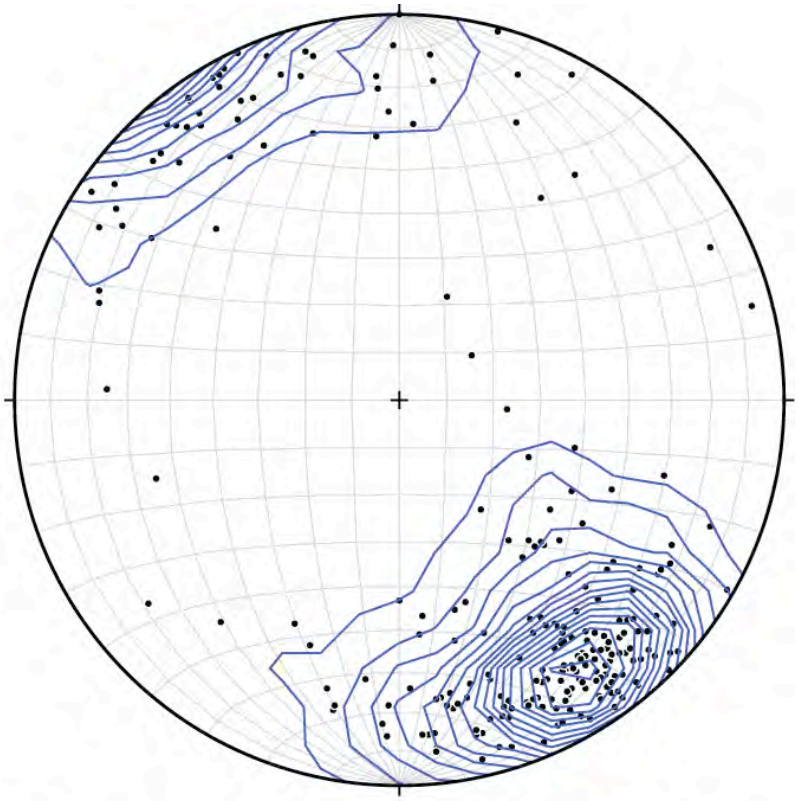

Figure 10. Stereonet plot of lineations in the study area (n=236).

however, northeast of Ross Dam folded foliation is present and defined by alternating lighter- and darker-colored bands.

Folds

Folds occur in 60 of the 255 outcrops studied during this research. Refolded folds occur in 9 of the 60 outcrops with folds. Most of the folds are in banded biotite gneiss, metapelite, and "metagraywacke." This pattern presumably reflects the much less well-developed rock anisotropy in the orthogneisses. Four generations of folds are expressed in the study area as described below.

First Fold Generation (F_3)

The earliest folds are isoclinal to tight and are only observed at the outcrop scale. Foliation, compositional layering, and leucosomes are folded. Wavelengths range from 2 to 22 cm, and folds have angular and slightly thickened hinges. Axial planes are inclined to recumbent (Fig. 11). The lower hemispheric stereonet plot of axial planes shows scatter that probably resulted from subsequent refolding. Variably oriented hinge lines plunge from 2º to 51º, mostly to the SE (Fig. 12).

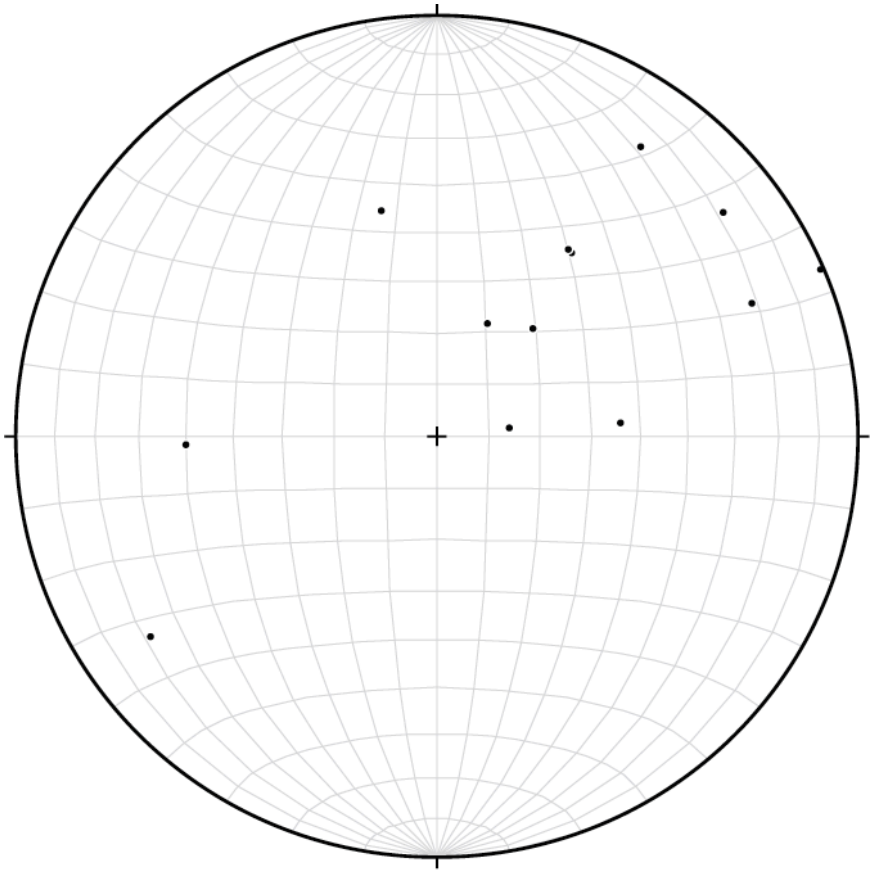

Figure 11. Stereonet plot of poles to F_3 axial planes (n=13).

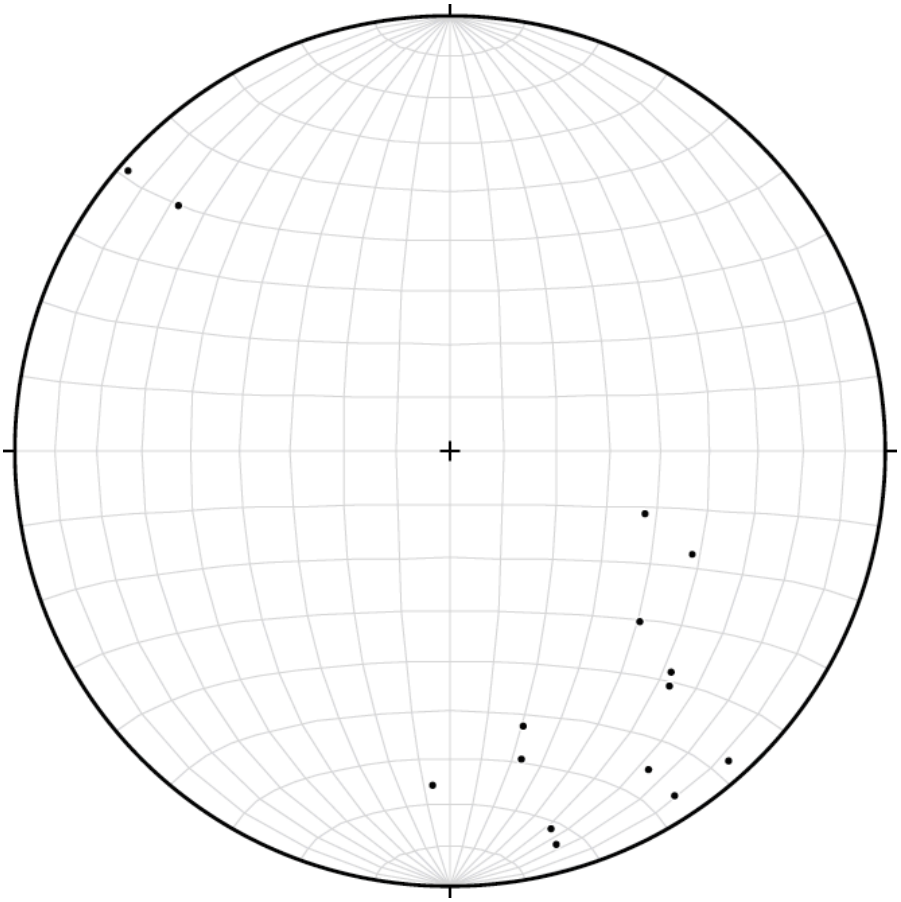

Figure 12. Stereonet plot of F_3 hinge lines (n=15).

Second Fold Generation (F_4)

Later folds are mostly open to gentle and thicknesses of layers change little between hinges and limbs indicating a nearly parallel (Class 1B) geometry. Wavelength ranges from outcrop scale (1-13 cm) to map scale (0.7 to 2.6 km; 1.3 km on average). The second generation folds are developed throughout the study area and are present in all rock types except the Diablo Lake orthogneiss, felsic dikes, and dacite dikes, which cut these folds. Refolded folds were observed at three outcrops on different ends of the study area in the banded biotite gneiss and "metagraywacke." Refolding of the first generation folds formed type 2 to type 3 interference patterns (Fig. 13). Axial planes of the second generation folds are upright to gently inclined and strike NW (Fig. 14). The poles to these axial planes form a girdle on a lower hemispheric stereographic projection; the pole to the girdle is 15º to 144º (Fig. 14). Hinge lines of the second generation folds plunge shallowly and almost exclusively to the SE, forming a moderate cluster of data points on a stereonet plot (Fig. 15). The pole to the girdle of all foliation measurements (19º to 150º; Fig. 9) is similar to the mean hinge line plunge and trend of the second fold generation (17º to 152º; Fig.15) strongly implying that the map-scale folds are second generation folds.

In order to evaluate the consistency of folding at different scales, outcrop- and intermediate-sized (2 km^2) areas were analyzed. The intermediate scale is represented by all foliation measurements from the Thunder Arm map area (Plate 2).

Figure 13. Refolded folds with type 2-3 interference patterns (note quarter for scale).

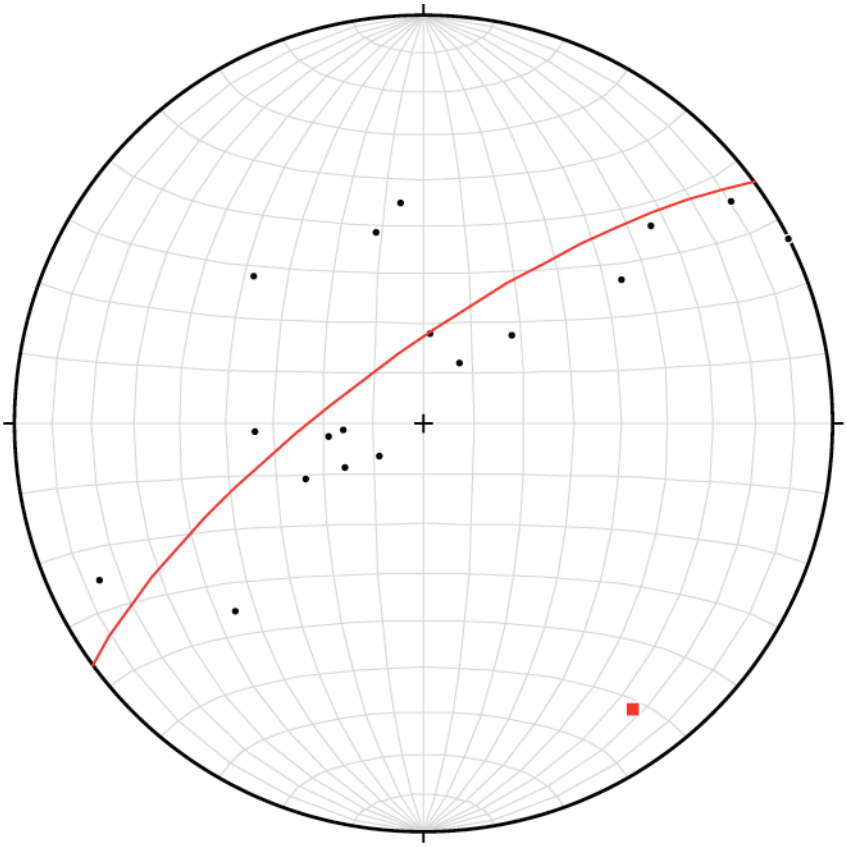

Figure 14. Stereonet plot of poles to F_4 axial planes (n=18). Pole to the girdle (red square) is 15º to 144º.

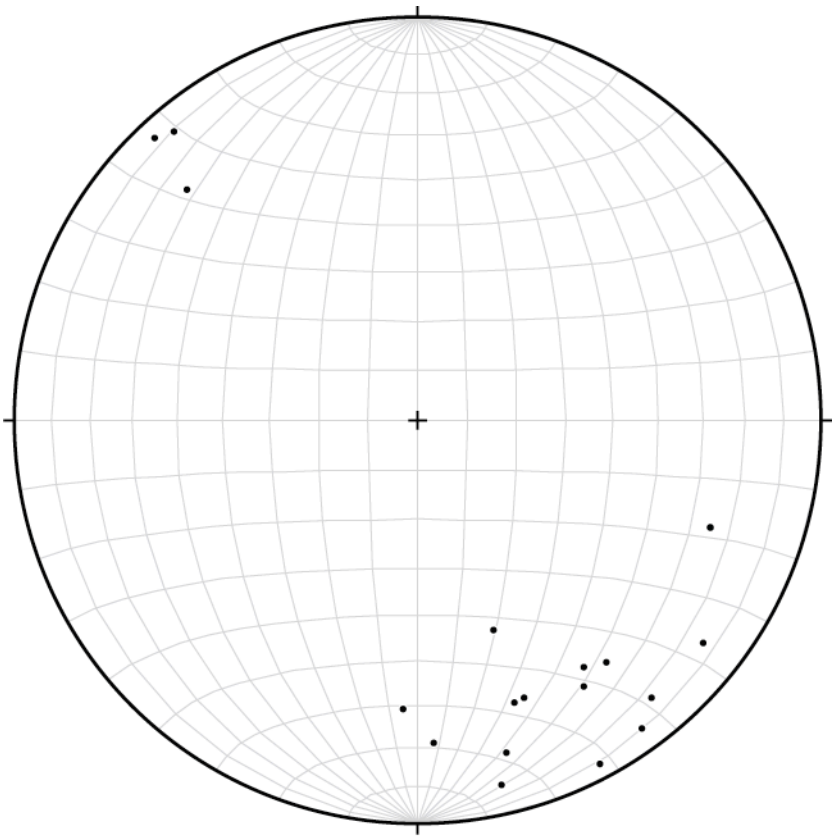

Figure 15. Stereonet plot of F_4 hinge lines (n=18).

The pole to the girdle of the foliations in this area is 17º to 155º and is consistent with the pole to the girdle for foliations in the entire study area (Fig. 16). The foliation plots of both the intermediate- and map-scale domains reveal NW and SE trending folds. The foliations in the intermediate-scale domain fit less tightly in a girdle than in the large map area. This observation suggests that the folds are less cylindrical in this intermediate-scale domain than elsewhere.

To assess fold consistency on a more detailed scale, a well-exposed antiformal hinge zone and adjacent limbs with a 75 m wavelength was studied in the central portion of the study area directly west of Thunder Arm (Fig. 17 and Plate 1). Foliation strikes NW and dips shallowly to steeply (Fig. 18). The pole to the girdle of the foliation measurements is 13º to 149º. Smaller wavelength (0.5 to 3 m) and amplitude (0.25 to 1 m) parasitic folds that have "S," "M," and "Z" geometries are also present (Fig. 18). The 75 m antiformal hinge zone is parasitic to the regional antiform as they have similar orientations and geometries. Thus, parasitic folds occur on both the kilometer and meter scale in the study area. Stereographic plots of the foliation measurements for the 75-m-wavelength fold (Fig. 18) are equivalent to those of the intermediate-sized area (Fig. 16) and the entire study area (Fig. 9); specifically, the poles to the girdles corresponding to the intermediate-scale and map-scale folds are similar (compare Figs. 9, 16, and 18). There is also consistency between outcrop-scale hinge line orientations and the poles to the girdle of the larger folds. In summary, orientations of the second fold generation are consistent at the map-, intermediate-, and outcrop-scale.

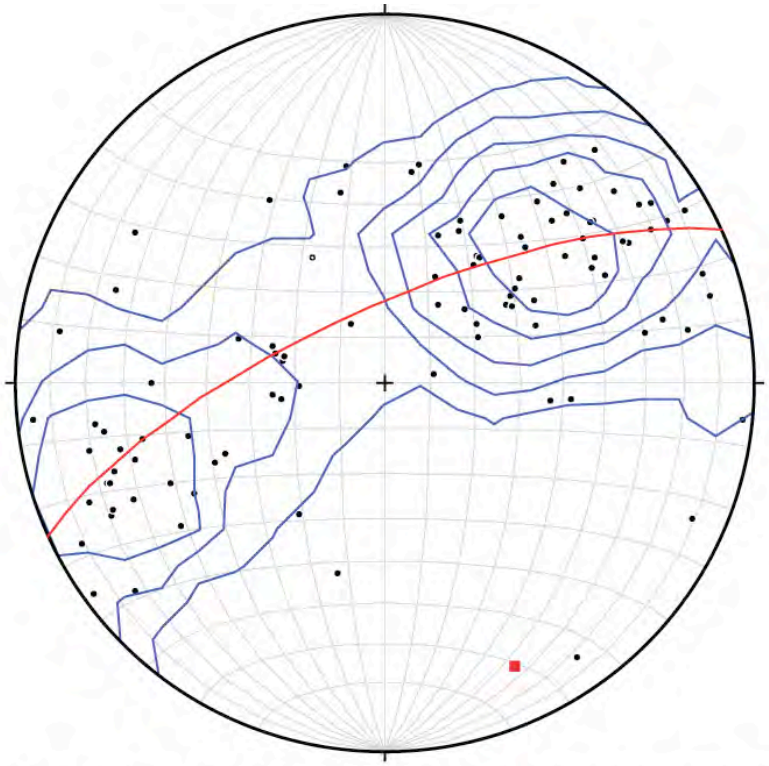

Figure 16. Stereonet plot of detailed map area foliation measurements (n=100). The pole to the girdle (red square) defined by foliations is 17° to 155°.

Figure 17. Photograph of the well-exposed hinge zone. Foliation strikes NW and dips shallowly to steeply. Smaller wavelength and amplitude folds within the hinge zone form S, M, and Z parasitic folds (traced with light green line).

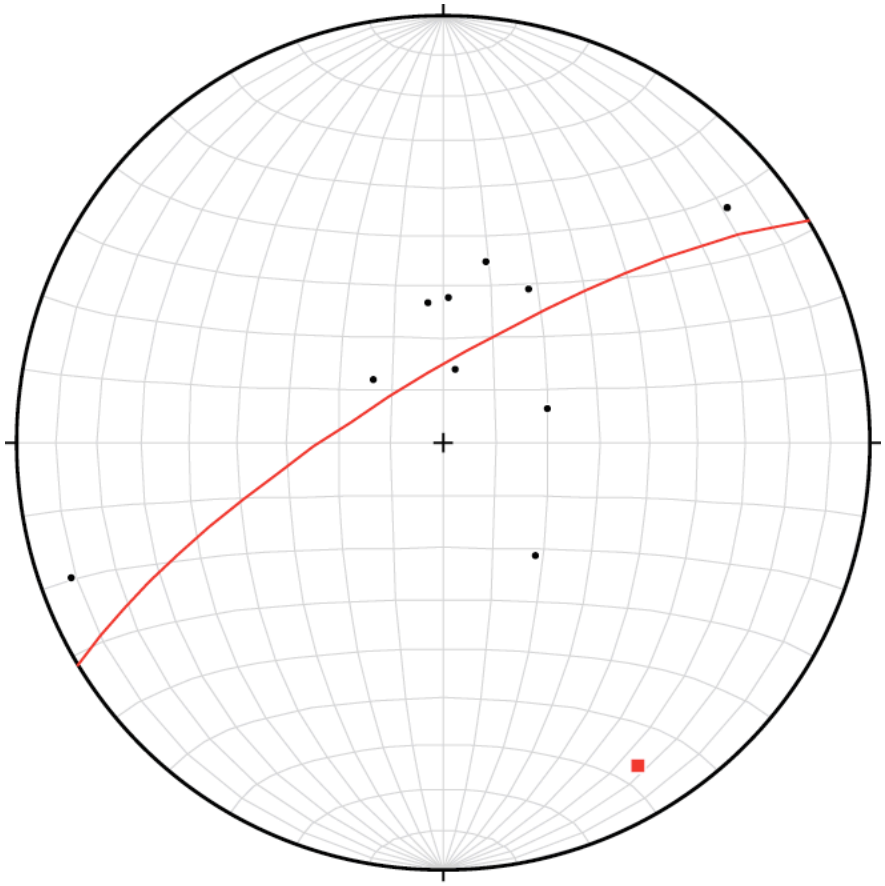

Figure 18. Stereonet plot of poles to hinge zone foliation measurements (n=10). Pole to the crude girdle (red square) is 13° to 149°.

Third Fold Generation (F_5)

The third fold generation is not seen in outcrop, but is inferred from the poles to the F_4 axial planes that plot moderately well in a girdle suggesting the axial planes were folded (Fig. 14). The pole to the girdle is 15º at 144º. The geometry and scale cannot be determined for these cryptic folds from stereonet projections.

Fourth (?) Fold Generation

A poorly-defined generation of late and very weak folds is suggested by the curvature of map-scale F_4 hinge lines. Crude estimates of wavelengths range from 0.5 to 1 km. The folds are open to gentle and indicate minimal shortening. Axial traces of these loosely constrained folds trend roughly NE-SW, which is about 90º from the other fold generations.

Microstructures

Kinematic Indicators

Thin sections were cut in the inferred X-Z plane of the strain ellipsoid (parallel to lineation and perpendicular to foliation) and analyzed to obtain detailed information about asymmetric microstructures that enable determination of sense-of-shear. Non-

coaxial shear is recorded by asymmetric microstructures from 52 localities in the study area. Banded biotite gneiss and paragneiss contain most of the kinematic indicators. Orthogneiss units contain 9 out of the 52 stations with consistent asymmetric microstructures.

Asymmetric microstructures used for kinematic analysis include the following: S-C fabrics, plagioclase porphyroclasts and garnet porphyroblasts with asymmetric biotite tails, biotite "fish," and oblique quartz foliation (Fig. 5). Asymmetric porphyroclasts and porphyroblasts, sigmoidal leucosomes bound by C-surfaces, and S-C fabrics are also recognized at the outcrop scale (Fig. 4) in 10 locations. At all of these locations, the outcrop- and thin-section analyses are in agreement. Biotite "fish," S-C fabrics, and sigmoidal porphyroclasts of plagioclase are the most abundant types of kinematic indicators (in descending order). The least abundant indicators are oblique quartz foliation, cummingtonite "fish," and delta-type rotated grains. Asymmetric leucosomes bounded by narrow shear surfaces range from 7 to 80 cm in width. Recrystallized biotite and quartz best define the C-surfaces. The average angle between S- and C-surfaces is 25º. The asymmetric porphyroclasts and porphyroblasts are almost exclusively sigmoidal; only 2 out of the 22 thin sections with asymmetric rotated grains are delta-type.

Dextral and sinistral shear are roughly equally developed. Their distribution does not fit a simple pattern. If it is assumed that asymmetric structures were folded along with foliation by the second fold generation, and if foliation is restored to roughly horizontal, kinematics can be evaluated based on their pre-folding orientation.

In this orientation, domains are apparent that trend roughly NW-SE; some of the domains record top-to-the-NW shear and others have top-to-the-SE shear (Fig. 19). Some of the domain boundaries are poorly constrained, and the domains do not correlate with rock types.

Deformation Temperature

Mineral microstructures are used to estimate temperature of deformation throughout the study area (Fig. 6). Assuming that strain rates did not vary drastically, ductile deformation overall probably occurred in two distinct regimes. Relatively low-temperature (300-400º C) and medium- to high-temperature (≥450º C) regimes are implied by the microstructures. It is more straightforward to assign temperatures for orthogneiss units, as metapelites and amphibolites were presumably deformed under amphibolite-facies conditions to form the dominant foliation. A few samples displaying higher-temperature deformation also contain lower-temperature microstructures such as undulatory extinction in quartz and bent or cracked plagioclase grains. These indicate overprinting probably occurred during or after significant exhumation and cooling of the gneiss complex. No samples examined in this study exhibit overprinting of lower-temperature microstructures by higher-temperature ones.

Samples with lower (n=22)- and higher (n=15)- temperature microstructures are apparently focused in different km-scale domains, although more data are needed

to refine the locations of the domain boundaries (Fig. 20). As with the kinematic domains, rock type and deformation temperature do not appear to correlate; deformation temperature domains transect unit contacts. The kinematic and deformation temperature domains, however, seemingly roughly correlate (Fig. 21). Specifically, 10 of the 14 lower-temperature microstructures correlate with the top-to-the-NW deformation, and 5 out of the 7 higher-temperature microstructures correlate with top-to-the-SE deformation. Top-to-the-SE shear is inferred to have occurred earlier, while the Skagit Gneiss Complex was near peak-metamorphic temperature. Deformation during and/or after subsequent cooling is postulated to have captured a change in the strain field to top-to-the-NW shear

DISCUSSION

Timing of Deformational "Episodes"

Interpretation of the timing of deformational "episodes" in the Skagit Gneiss Complex and younger intrusive units is based on field and microscopic observations and zircon and monazite U-Pb dates. Separating out "episodes" of deformation facilitates analysis of the complex history of these rocks. This approach is not

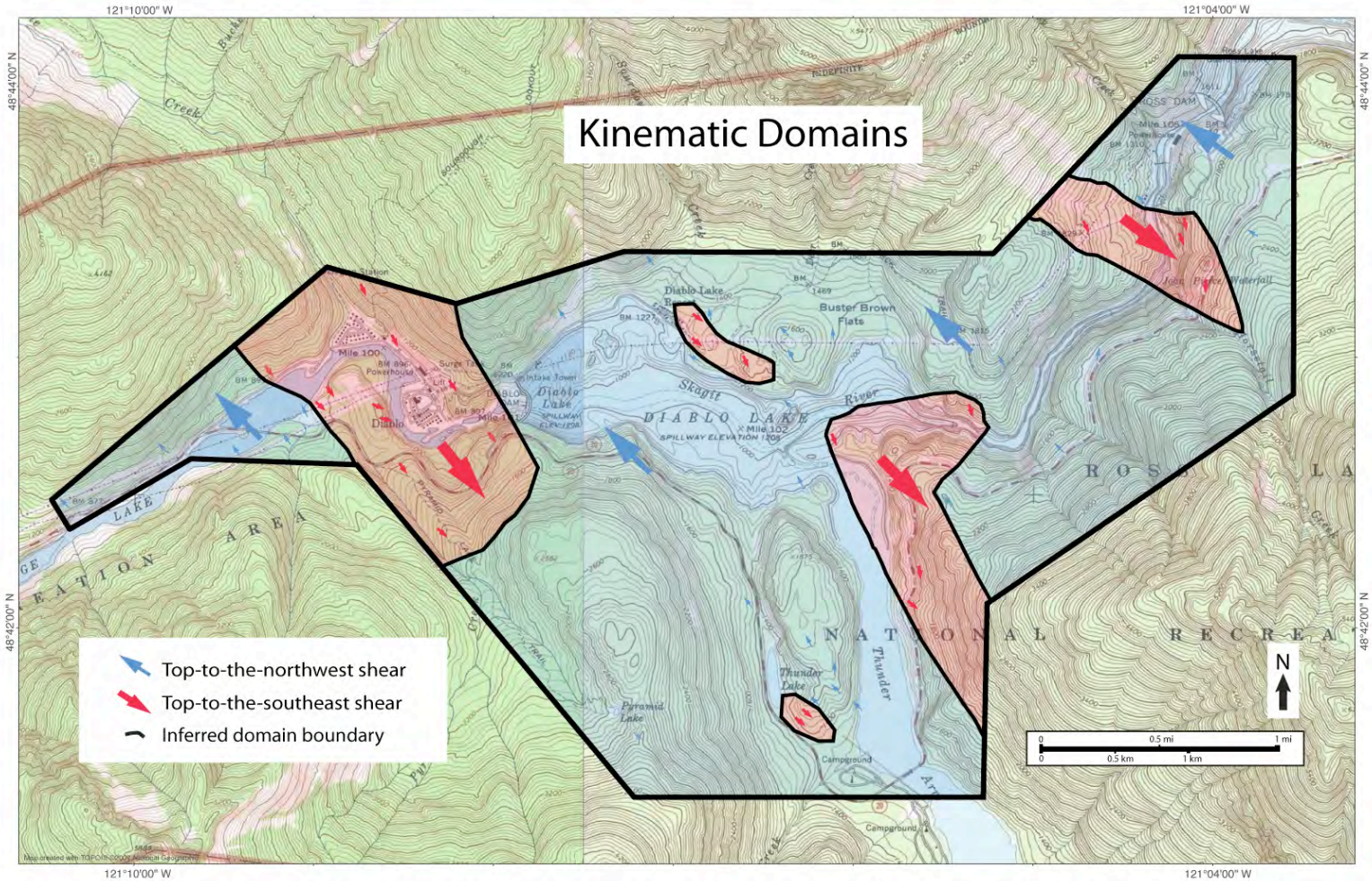

Figure 19. Sense-of-shear indicators. Small arrows represent individual locations where sense-of-shear was determined, and inferred domains with different sense-of-shear are indicated.

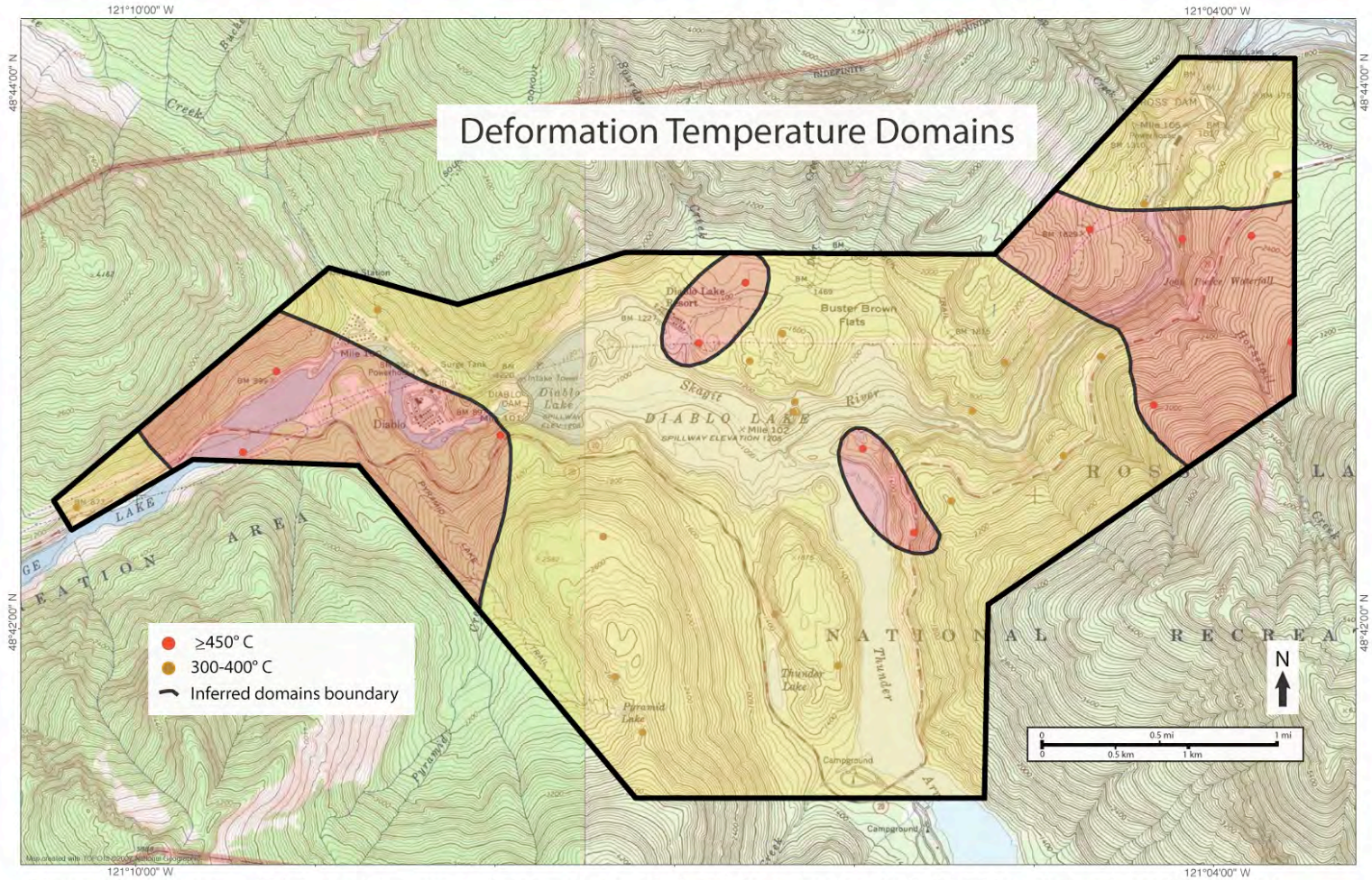

Figure 20. Lower- and higher-temperature microstructures. Colored dots represent individual locations where deformation temperature was determined.

intended to convey that structures formed simultaneously throughout the study area or that there were necessarily sharp temporal gaps between "episodes." For example, folds from the F_3 deformational "episode" may have formed earlier in the western part than in the eastern part of the study area. Also, plutons emplaced at different times would record different lengths of deformational history. "Episode," for the purposes of this analysis, is defined on the basis of the sequence of structures observed in different parts of the study area (e.g., foliation, lineation, or folds). Although each deformational "episode" is probably time transgressive and spatially variable, the "episode" concept allows for a simpler treatment of the structural data collected in this study. Quotations are used to acknowledge the simplistic nature of this treatment.

Number assignments for each deformational "episode" build on the numbering scheme of Haugerud et al. (1991). The earliest foliation (S_1) and lineation (L_1) were recognized in amphibolite xenoliths within an orthogneiss body on Custer Ridge north of the study area in British Columbia (Haugerud et al., 1991). S_1 and L_1 were not recognized in the study area, hence, the earliest deformational "episode" is D_2.

There are five main ductile structural "episodes" recorded in the study area that are described from oldest to youngest (Table 1). The main foliation and lineation, which represent the oldest recorded deformation (D_2), are well developed in all units except the Diablo Lake orthogneiss, felsic dikes, and dacite dikes. Leucosomes, that

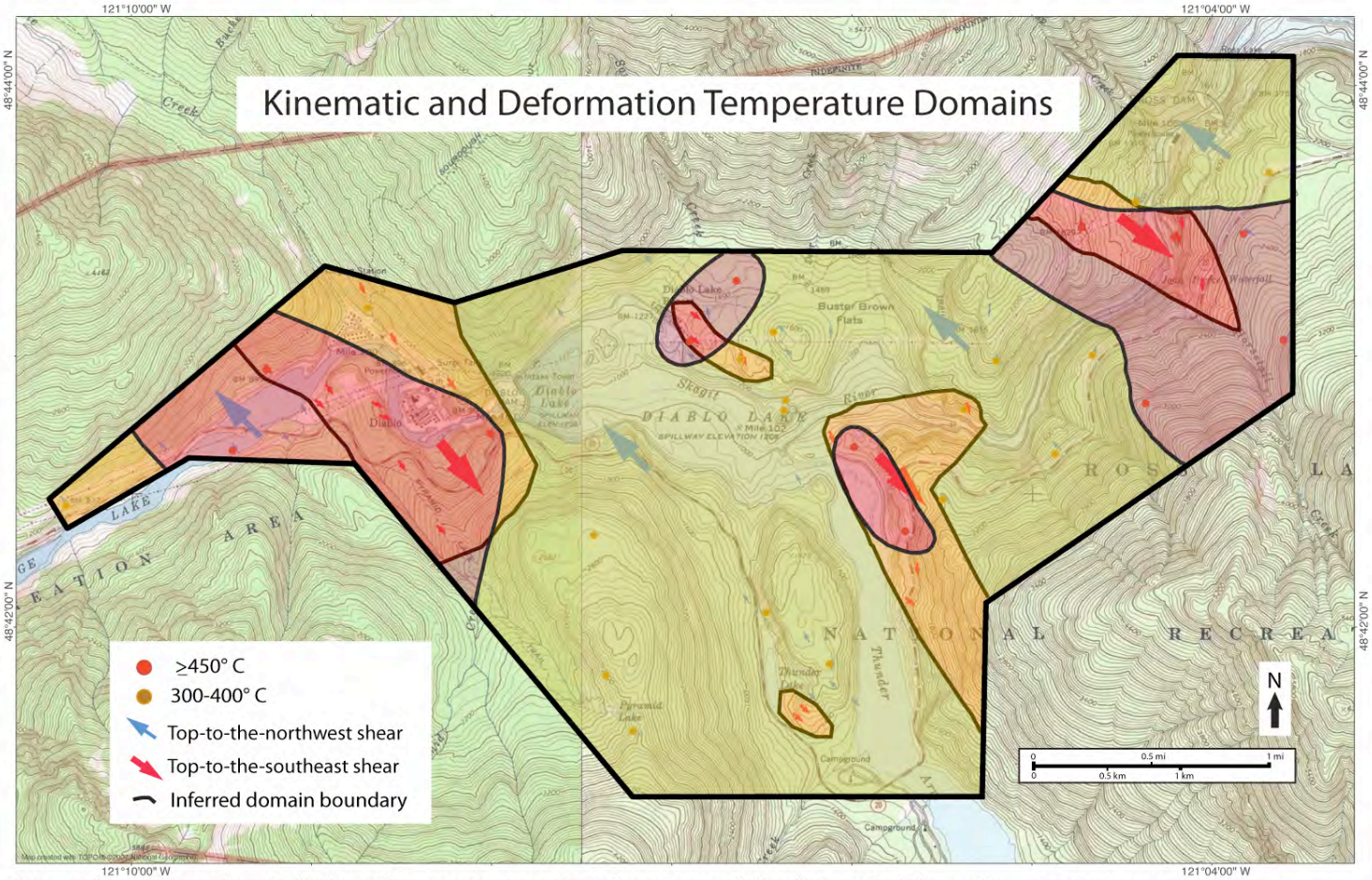

Figure 21. Kinematic and deformation temperature domains. A correlation between deformation temperature and sense-of-shear is suggested.

cut the foliated units, yield U-Pb zircon dates of 69-63 and 54-51 Ma (Gordon, 2009) from the western and eastern margins of the study area, respectively. The dates from the younger leucosomes that contain the main foliation and lineation (S_2 and L_2), indicate that D_2 deformation probably at least in part during regional transtension. indicate that D_2 deformation probably occurred at least in part during regional transtension.

Leucosomes are strongly to weakly foliated and lineated and generally share the same fabric as their hosts. Partially melting rocks are weak and should deform readily. Host rocks may thus have been actively deforming when leucosomes were also injected, and their shared fabric indicates that the leucosomes and host rocks were deformed together. The timing of deformation in older rocks that record multiple deformation sequences is less clear.

Table 1: Ductile deformational "episodes" in the study area.

Number	**Deformational "Episode"**	**Date**
D_2	Main Foliation and Lineation (S_2=L_2)	≥69-51 Ma
D_3	First Fold Generation (F_3)	≥51-46 Ma
D_4	Second Fold Generation (F_4)	≥51-46 Ma
D_5	Third Fold Generation (F_5)	≥51-46 Ma
D_6	Strong Constrictional Fabric (L_6>>S_6)	46-≥34 Ma

The earliest folds only fold the main foliation and lineation. The second generation folds the first generation and migmatitic leucosomes as seen in outcrop and map pattern (Figs. 13 and 17). Folds of the third generation are similarly oriented to earlier folds. The latest and fourth-generation (?) folds have crude NE-SW axial traces, which are about 90º from the previous fold generation. The NW-SE shortening has not been recognized in the Cascades core outside of the Skagit Gneiss Complex and its significance is uncertain.

The 46-45 Ma Diablo Lake orthogneiss cuts all fold generations and provides a younger limit for folding (e.g., Misch, 1968). At the western edge of the study area, leucosomes in folded metapelite yield dates inferred to represent melt crystallization at 69-63 Ma (Gordon, 2009). Folding of the meta-supracrustal rocks probably initiated prior 51 Ma. Regional strain during the mid-Cretaceous was shortening and/or transpression that affected much of the Cascades core and flanking lower-grade rocks (Fig. 1); therefore, it is likely that the folds formed under these boundary conditions (e.g., Misch, 1966, 1988; Brown, 1987; Miller et al., 2006). However, there are no dates or field relations that directly demonstrate folding before 51 Ma.

The second and third fold generations likely formed during regional dextral transtension postulated to have begun at 57 Ma and continuing to at least 45 Ma (e.g., Johnson, 1985; Miller and Bowring, 1990; Haugerud et al., 1991). The timing of the fold generations are not well constrained, but at least some folding occurred during the transtensional regime. Folds can form during transtension but probably do not produce much shortening on a regional scale (Dewey, 2002). In the study area at least

32% shortening is recorded by the second fold generation. Upright folds in the southern part of the Skagit Gneiss Complex record at least 25% shortening (Shea, 2008). Parts of the Swauk basin, 155 km south of the study area, were also shortened by at least 25 to 30% in the Eocene (Doran, 2009). Thus, the magnitude of Eocene shortening by the second fold generation within the study area is consistent with known Eocene shortening in other parts of the Skagit Gneiss Complex and Swauk basin and suggests at least a short interval of regional shortening during an extended period of overall transtension.

Leucosomes within orthogneisses, particularly the hornblende-cummingtonite-garnet orthogneiss with an inferred crystallization age of 68 Ma, are minimally folded compared to those in better-layered units. This pattern may indicate that migmatization mostly postdated folding in some locations. More likely, the lack of folds indicates that the rheologically strong orthogneiss bodies shielded the leucosomes from folding. Within the banded biotite gneiss, leucosomes are locally boudinaged and thus were more competent than their host during deformation.

The latest ductile deformation observed in the study area is the lineation-dominated constrictional fabric (L_6) in the 46-45 Ma Diablo Lake orthogneiss. The Chilliwack batholith that cuts the Skagit Gneiss Complex to the northwest is dated at 34 Ma and constrains the last deformational episode (Fig. 2). The lineation in the Diablo Lake orthogneiss is oriented similarly to the main lineation in older rocks. Stretching direction thus most likely remained roughly constant during all of the deformational "episodes." During deformation of the Diablo Lake orthogneiss,

subvertical shortening was accompanied by subhorizontal shortening. This late strain might have been partitioned into the relatively warmer and weaker Diablo Lake orthogneiss.

An undated dacite dike, mapped directly northeast of Thunder Knob, cuts banded biotite gneiss. It shows no significant ductile deformation and caps the ductile deformational history recorded in the study area.

Kinematic Indicators, Deformation Temperatures, and Folds

Combining various data for the study area reveals a number of correlations and patterns. Sense-of-shear and deformation temperature broadly correspond. Specifically, top-to-the-NW shear occurs mostly in the lower-temperature (300-400º C) deformation domains, and top-to-the-SE shear correlates mostly with higher-temperature (≥450º C) domains.

In one scenario, the position of the top-to-the-NW and top-to-the-SE domains reflects structural level. This scenario is unlikely as there is only limited structural thickness exposed in the study area and no regional strain gradient or decollement has been recognized.

Exhumation of the Skagit Gneiss Complex probably occurred during the Eocene (Wernicke and Getty, 1997) and decompression from 8-10 to 3-5 kbar was nearly isothermic between 725-600º C (Whitney, 1992a). Some high-temperature

microstructures are visible in thin section and may have formed during initial exhumation but before significant cooling. For example, recrystallized cummingtonite is found in the C-surfaces in three samples and formed at temperatures of ≥500º C (Passchier and Trouw, 2005), and additional microstructures record a moderate- to high-temperature (≥450º C), as described above. These microstructures may have formed before, during, or after exhumation, as the Skagit Gneiss Complex remained hot during initial near-isothermal decompression. Lower-temperature (300-400º C) microstructures probably occurred after significant exhumation.

Distribution and Timing of Intrusions and Migmatites

Contacts of the moderately to slightly foliated orthogneiss bodies are mostly concordant to foliation. This pattern may indicate concordant emplacement or that contacts were rotated into parallelism with the surrounding host rock as a result of progressive deformation. The only moderate to weak strength of foliation and lineation probably precludes major rotation of contacts and thus these orthgneisses were likely emplaced concordantly as sills. Subsequent younger deformation and lack of diagnostic criteria make it difficult to determine if pluton emplacement was syntectonic.

Deformation temperature can offer insight into timing of pluton emplacement. The hornblende orthogneiss in the northeastern portion (Plates 1-3) of the study area

contains three stations with lower-temperature microstructures (300-400º C) and no higher-temperature microstructures (≥450º C) were recognized, which is compatible with emplacement after some exhumation of the Skagit Gneiss Complex. The younger Diablo Lake orthogneiss also contains only lower-temperature microstructures.

Migmatite distribution within the study area could be influenced by folding. The Skagit Gneiss Complex is in the core of a regional antiform, and the center of the main antiform contains the highest concentration of leucosomes according to Tabor and Haugerud (1999, Fig. 53). This pattern may result from originally subhorizontal isotherms, which led to depth-controlled partial melting at deeper structural levels. Upright folding then brought these deeper levels up in the core of antiforms. In detail, this interpretation is undoubtedly too simple for three main reasons. Migmatites formed at more than one time interval (Gordon, 2009), bulk rock composition presumably influenced distribution of migmatites, and multiple migmatite types are developed in the study area (Misch, 1968; Yardley, 1978; Whitney, 1992b).

General Implications for Cascades Core

The data collected from this study of the northern part of the Skagit Gneiss Complex combined with other recently completed work 40 km and 65 km to the southeast (Michels, 2008; Shea, 2008) offer insights into the structure of the Skagit

Gneiss Complex as a whole. In the southern (Shea, 2008) and northern portions (this study) of the complex, foliation strikes NW with variable dips. In contrast, foliation in the central part of the complex mainly strikes N-S to NNE with variable dips (Michels, 2008). Lineations in the northern and southern sections plunge moderately to shallowly to the SE (Shea, 2008); however, lineations in the central Skagit Gneiss Complex plunge shallowly to the NNE (Michels, 2008). These data suggest that the NW-striking foliation and shallow to moderately SE plunging lineation are the dominant fabrics for the Skagit Gneiss Complex, and that foliation and lineation are deflected in the central section.

Four fold generations are recorded in the southern part of the Skagit Gneiss Complex (Shea, 2008) and four (although not identical) fold generations are recorded in the northern part as described above. The F_4 folds in the north and south are upright and plunge shallowly, and they likely represent the same deformation. Upright folds are much less common in the central part of the complex (Michels, 2008).

Traced from the southern end of the gneiss complex northward, the foliation strike swings over a distance of 25 km from WNW to NW to NNE and then over a distance of 40 km back to a NW orientation in the study area (Miller, 1987; Miller and Bowring, 1990; Michels, 2008; Shea, 2008; R.B. Miller, unpublished data). This regional fold is tens of kilometers in wavelength and has a steep NE striking axial plane and a steep plunge (Shea et al., 2007). It represents the youngest folding on a regional scale within the complex (Shea, 2008). The fourth and probably youngest fold generation proposed for the study area may correlate with the large regional fold.

The sense of non-coaxial shear, similar to the foliation and lineation in the Skagit Gneiss Complex, are also homologous in the northern and southern portions but differ in the center. Both top-to-the-NW and -SE shear are present in the north and south, whereas mostly top-to-the-N shear domains occur in the central part of the complex (Michels, 2008). Deformation temperature is 300-400º C or ≥450º C in the north and south, but the central section mainly records only higher-temperature deformation of 400-650º C (Michels, 2008; Shea, 2008; this study). Top-to-the-NW shear probably correlates with the low-temperature deformation, and top-to-the-SE motion with the medium to high-temperature deformation in both the northern and southern parts of the Skagit Gneiss Complex. Shea (2008) postulated that the change in shear direction is coincident with the regional change from transpression to transtension at 57 Ma. In summary, the northern and southern portions of the gneiss complex have similar orientations of structures and deformational history, but the central portion differs in some important aspects and its structure is enigmatic (see Michels, 2008).

Eocene deformation in the crystalline core is both brittle and ductile (e.g., Tabor et al., 1989; Miller et al., 2009a). Deformation in the brittle crust is accommodated by numerous high-angle map-scale fault systems, including the Straight Creek-Fraser fault, Entiat fault, Foggy Dew fault, and Ross Lake fault (Figs. 1 and 2). Also, dike swarms in both the Eocene Swauk basin and Cascades core imply WNW-ESE to NW-SE stretching (Miller et al., 2009a). South of the study area, Eocene ductile deformation was accommodated in part by the Dinkelman decollement

(Fig. 2), which separates Late Cretaceous Swakane Gneiss in the footwall from the Napeequa unit and 91-72 Ma arc plutons in the hanging wall. Motion on the decollement and pervasive non-coaxial shear in the Swakane Gneiss are top-to-the-N, which is slightly oblique to the orogen (Paterson et al., 2004; Miller et al., 2009a). The latest motion on the Dinkelman decollement is likely extensional, as indicated by differences in Ar/Ar cooling ages, and displacement probably continued until around 48 Ma (Matzel et al., 2004; Paterson et al., 2004). The top-to-the-N displacement on the Dinkelman decollement, the orogen-parallel NW stretching indicated by lineation-dominated fabric in the study area, and the top-to-the-NW shear in the Skagit Gneiss Complex roughly correspond temporally. The differing stretching directions of the shallow and deep crust suggest some degree of decoupling during deformation (Miller et al., 2009b).

CONCLUSIONS

1. Older orthogneiss (>46 Ma) is delineated into three units by location and mineral modes (occurrence of garnet, cummingtonite, and/or hornblende).
2. Metapelite occurs in two newly-discovered localities.
3. Felsic and dacite dikes cut the Skagit Gneiss Complex.
4. The main foliation and lineation (D_2) mostly formed from ≥69 to 51 Ma.
5. The earliest mesoscopic folds are isoclinal to tight with wavelengths ranging from 2 to 22 cm; hinges are slightly thickened and angular. Axial planes are inclined to recumbent, and hinge lines plunge from 2º to 51º, mostly to the SE.
6. The second generation of folds are outcrop- to map-scale, upright, open to gentle, and parasitic to the regional antiformal structure of the gneiss complex. Hinge lines plunge shallowly and almost exclusively to the SE. Refolding of the first generation folds formed type 2 to type 3 interference patterns. The second generation folds likely formed between 51 and 46 Ma.
7. The third generation of folds are inferred from the poles to the F_4 axial planes that plot moderately well in a girdle. The pole to the girdle is 15º to 144º.
8. A fourth and youngest fold generation is postulated based on the curvature of map-scale hinge lines. Folds are open to gentle with wavelengths ranging from 0.25 to 1 km, and crude axial traces trend roughly NE-SW.

9. Kinematic indicators at the micro- and mesoscale give top-to-the-NW and top-to-the-SE sense-of-shear. Km-scale domains recording the same sense-of-shear broadly trend NW-SE across the study area.
10. Deformation of the gneiss complex can be broken into lower-temperature (300-400º C) and medium- to higher-temperature (≥450º C) regimes. Top-to-the-NW-directed shear correlates with the lower-temperature deformation (300-400º C) and top-to-the-SE-directed shear correlates with higher-temperature deformation (≥450º C).
11. At least two of the four fold generations formed from 51 to 46 Ma and suggest an interval of shortening during an overall transtensional strain regime.
12. Late lineation-dominated fabric preferentially imprinted on the Diablo Lake orthogneiss, and is bracketed between 46-34 Ma.
13. Migmatitic leucosome outcrop volumes plot in higher, moderate, and lower (>20%, 20-5%, and <5%) domains.
14. Foliation, lineation, folds, shear sense, and deformation temperatures in the northern and southern portions of the Skagit Gneiss Complex are similar, but the central portion differs significantly.

REFERENCES CITED

Babcock, R.S., and Misch, P., 1988, Evolution of the crystalline core of the North Cascades range, *in* Ernst, W.G., ed., Metamorphism and crustal evolution of the western United States: Rubey Volume 7, Prentice Hall, New Jersey, p. 214-232.

Babcock, R.S., Armstrong, R.L., and Misch, P., 1985, Isotopic constraints on the age and origin of the Skagit Metamorphic Suite and related rocks: Geological Society of America Abstracts with Programs, v. 17, no. 6, p. 339.

Brandon, M.T., Cowan, D.S., and Vance, J.A., 1988, The Late Cretaceous San Juan thrust system, San Juan Islands, Washington: A case history of terrane accretion in the western Cordillera: Geological Society of America Special Paper 221, 88 p.

Brown, E.H., 1987, Structural geology and accretionary history of the Northwest Cascades system, Washington and British Columbia: Geological Society of America Bulletin, v. 99, p. 201-214.

Brown, E.H., and Walker, N.W., 1993, A magma-loading model for Barrovian metamorphism in the southeast Coast Plutonic Complex, British Columbia and Washington: Geological Society of America Bulletin, v. 105, p. 479-500.

Clay, P.J., and Miller, R.B., 2008, Brittle structures in the Ross Lake National Recreation Area, North Cascades, Washington: Geological Society of America Abstracts with Programs, v. 40, no. 1, p. 66.

Dewey, J. F., 2002, Transtension in arcs and orogens: International Geology Review, v. 44, p. 402-439.

Doran, B., 2009, Structure of the Swauk Formation and Teanaway dike swarm, Washington Cascades [M.S. thesis]: San Jose, California, San Jose State University, 97 p.

Evans, B.W., and Davidson, G.F., 1999, Kinetic control of metamorphic imprint during synplutonic loading of batholiths: An example from Mt. Stuart, Washington: Geology, v. 27, p. 129-139.

Geschwind, C.-H., and Rutherford, M.J., 1992, Cummingtonite and the evolution of the Mount St. Helens (Washington) magma system: An experimental study: Geology, v. 20, p. 1011-1014.

Gordon, S.M., 2009, Timescales of migmatization, metamorphism, and deformation in a collapsed orogenic plateau [Ph.D. thesis]: Minneapolis, Minnesota, University of Minnesota, 379 p.

Haugerud, R.A., van der Heyden, P., Tabor, R.W., Stacey, J.S., and Zartman, R.E., 1991, Late Cretaceous and early Tertiary plutonism and deformation in the Skagit Gneiss Complex, North Cascade Range, Washington and British Columbia: Geological Society of America Bulletin, v. 103, p. 1297-1307.

Hoppe, W.J., 1984, Origin and age of the Gabriel Peak orthogneiss, North Cascades, Washington [M.S. thesis]: Lawrence, Kansas, University of Kansas, 79 p.

Johnson, S.Y., 1985, Eocene strike-slip faulting and nonmarine basin formation in

Washington: Society of Economic Paleontologists and Mineralogists Special Publication, v. 37, p. 283-302.

Kamb, W.B., 1959, Petrofabric observations from Blue Glacier, Washington, in relation to theory and experiment: Journal of Geophysical Research, v. 64, p. 1891-1909.

Mattinson, J.M., 1972, Ages of zircons from the Northern Cascade Mountains, Washington: Geological Society of America Bulletin, v. 83, p. 3769-3783.

Matzel, J.P., Bowring, S.A., and Miller R.B., 2004, Protolith age of the Swakane Gneiss, North Cascades, Washington: Evidence of rapid underthrusting of sediments beneath an arc: Tectonics, v. 23, no. 6, p. TC6009, doi:10.1029/2003TC001577.

McGroder, M.F., 1991, Reconciliation of two-sided thrusting, burial metamorphism, and diachronous uplift in the Cascades of Washington and British Columbia: Geological Society of America Bulletin, v. 103, p. 189-209.

Michels, Z.D., 2008, Structures of the central Skagit Gneiss Complex, North Cascades, Washington [M.S. thesis]: San Jose, California, San Jose State University, 95 p.

Miller, R.B., 1987, Geology of the Twisp River-Chelan Divide region, North Cascades, Washington: Washington Division of Geology and Earth Resources Open File Report 87-17, 12 p., 12 pl.

Miller, R.B., and Bowring, S.A., 1990, Structure and chronology of the Oval Peak batholith and adjacent rocks: Implications for the Ross Lake fault zone, North

Cascades, Washington: Geological Society of America Bulletin, v. 102, p. 1361-1377.

Miller, R.B., and Paterson, S.R., 2001, Influence of lithological heterogeneity, mechanical anisotropy, and magmatism on the rheology of an arc, North Cascades, Washington: Tectonophysics, v. 342, p. 351-370.

Miller, R.B., Paterson, S.R., Lebit, H.A., Alsleben, H., and Luneberg, C., 2006, Significance of composite lineations in the mid- to deep crust: A case study from the North Cascades, Washington: Journal of Structural Geology, v. 28, p. 302-322.

Miller, R.B., Gordon, S.M., Bowring, S.A., Doran, B.A., McLean, N.M., Michels, Z.D., Shea, E.K., Whitney, D.L., Wintzer, N.E., and Mendoza, M.K., 2009a, Linking deep and shallow crustal processes in an exhumed continental arc, North Cascades, Washington, *in* O'Connor, J.E., Dorsey, R.J., and Madin, I.P., eds., Volcanoes to vineyards: Geologic field trips through the dynamic landscape of the Pacific Northwest: Geological Society of America Field Guide 15, p. 373-406.

Miller, R.B., Paterson, S.R., and Matzel, J.P., 2009b, Plutonism at different crustal levels: Insights from the 5–40 km (paleodepth) North Cascades crustal section, Washington, *in* Miller, R.B., and Snoke, A.W., eds., Crustal cross sections from the western North American Cordillera and elsewhere: Implications for tectonic and petrologic processes: Geological Society of America Special Paper 456, p. 125-149, doi:10.1130/2009.2456(05).

Misch, P., 1966, Tectonic evolution of the Northern Cascades of Washington State: A west-Cordilleran case history, *in* Gunning, H.C., ed., Symposium on the tectonic history and mineral deposits of the western Cordillera in British Columbia and neighboring parts of United States: Canadian Institute of Mining and Metallurgy, Special Volume 8, p. 101-148.

Misch, P., 1968, Plagioclase compositions and non-anatectic origin of migmatitic gneisses in Northern Cascade Mountains of Washington State: Contributions to Mineralogy and Petrology, v. 17, p. 1-70.

Misch, P., 1977, Bedrock geology of the North Cascades, *in* Brown, E.H., and Ellis, R.C., eds., Geological excursions in the Pacific Northwest: Bellingham, Washington, Guidebook Geological Society of America Annual Meeting, Western Washington University, p. 1-62.

Misch, P., 1988, Tectonic and metamorphic evolution of the North Cascades: An overview, *in* Ernst, W.G., ed., Metamorphism and crustal evolution of the western United States: Rubey Volume 7, Upper Saddle River, New Jersey, Prentice Hall, p. 179-195.

Passchier, C.W., and Trouw, R.A.J., 2005, Microtectonics, 2nd Edition: Berlin, Springer-Verlag, 366 p.

Paterson, S.R., Miller, R.B., Alsleben, H., Whitney, D.L., and Hurlow, H., 2004, Driving mechanism for >40 km of exhumation during contraction and extension in a continental arc, Cascades core, Washington: Tectonics, v. 23, p. 1-30.

Shea, E.K., 2008, Structural geology of the southern Skagit Gneiss Complex, North Cascades, Washington [M.S. thesis]: San Jose, California, San Jose State University, 90 p.

Shea, E.K., Miller, R.B., Michels, Z.D., and McLean, N.M., 2007, Structural Geology of the Skagit Gneiss Complex (SGC), North Cascades, Washington: Geological Society of America Abstracts with Programs, v. 39, no. 4, p. 10.

Stowell, H.H., and Stein, E., 2005, The significance of plagioclase-dominant coronas on garnet, Wenatchee block, Northern Cascades, Washington, USA: Canadian Mineralogist, v. 43, p. 367-385.

Tabor, R.W., and Haugerud, R.A., 1999, Geology of the North Cascades, a mountain mosaic: Seattle, Washington, The Mountaineers, 144 p.

Tabor, R.W., Haugerud, R.A., and Miller, R.B., 1989, Accreted terranes of the North Cascades Range, Washington: International Geological Congress Trip T307: American Geophysical Union, 62 p.

Tabor, R.W., Haugerud, R.H., Brown, E.H., and Babcock, E.H., 2003, Geologic map of the Mount Baker 30- by 60-Minute Quadrangle, Washington: Geologic Investigations Series I-2660, scale 1:100,000, 2 sheets.

Tepper, J.H., 1996, Petrology of mafic plutons associated with calc-alkaline granitoids, Chilliwack batholith, North Cascades, Washington: Journal of Petrology, v. 37, p. 1409-1436.

Walker, N. W., and Brown, E. H., 1991, Is the southeast Coast Plutonic Complex the

consequence of accretion of the Insular superterrane? Evidence from zircon geochronometry in northern Washington Cascades: Geology, v. 19, p. 714-717.

Wernicke, B., and Getty, S.R., 1997, Intracrustal subduction and gravity currents in the deep crust: Sm-Nd, Ar-Ar, and thermobarometric constraints from the Skagit Gneiss Complex, Washington: Geological Society of America Bulletin, v. 109, p. 1149-1166.

Whitney, D.L., 1992b, Origin of CO_2-rich fluid inclusions in leucosomes from the Skagit migmatites, North Cascades, Washington, USA: Journal of Metamorphic Geology, v. 10, p. 715-725.

Whitney, D.L., 1992a, High-pressure metamorphism in the Western Cordillera of North America: an example from the Skagit Gneiss, North Cascades, Washington, USA: Journal of Metamorphic Geology, v. 10, p. 71-85.

Whitney, D.L., and McGroder, M.F., 1989, Cretaceous crustal section through the proposed Insular-Intermontane suture, North Cascades, Washington: Geology, v. 17, p. 555-558.

Yardley, B.W.D., 1978, Genesis of the Skagit Gneiss migmatites, Washington, and the distinction between possible mechanisms of migmatization: Geological Society of America Bulletin, v. 89, p. 941-951.